DEUTSCHES ELEKTRONEN – SYNCHROTRON

DESY 91-074
July 1991

High-Energy Behaviour in a Non-Abelian Gauge Theory (III). Multiple Discontinuities and Particle →Multireggeon Vertices

J. Bartels

II. Institut für Theoretische Physik, Universität Hamburg

ISSN 0418-9833

NOTKESTRASSE 85 · D-2000 HAMBURG 52

To be sure that your preprints are promptly included in the
HIGH ENERGY PHYSICS INDEX,
send them to the following (if possible by air mail):

DESY
Bibliothek
Notkestrasse 85
D–2000 Hamburg 52
Germany

DESY 91-074
July 1991

ISSN 0418-9833

High-Energy Behaviour in a Non-Abelian Gauge Theory (III). Multiple Discontinuities and Particle → Multireggeon Vertices

J.Bartels

II. Institut für Theoretische Physik, Universität Hamburg, Germany

ABSTRACT

The high energy limit (Regge limit) of a spontaneously broken SU(2) gauge theory is studied beyond the leading-lns approximation. Calculations are based upon the analytic structure of scattering amplitudes in generalized Regge limits, and the resulting amplitudes satisfy reggeon unitarity in the t-channel as well as unitarity in the s-channel. The calculations lead to a sytematic construction of a reggeon field theory.

1 Introduction

Several years ago [1,2] (these two papers will henceforth be referred to as I and II) we have begun a program which tries to extract the high energy behavior in the Regge Limit of QCD. The calculations started from a spontaneously broken Yang-Mills theory (for simplicity, we used SU(2)) and were based upon the observation that the gauge boson reggeizes: for the leading lns approximation it was then verified that the analytic structure of multiparticle scattering amplitudes together with other elements of Regge theory [3] could be used to construct first elements of a complete reggeon field theory. It has also been known for many years that this leading-lns approximation in the vacuum exchange channel leads to a finite answer when the mass of the vector particle is taken to zero: this observation gave rise to the hope that the calculation done in a Higgs model might also be used for QCD: at least on the perturbative level calculations that are done in QCD agree with the conclusions from the Higgs model.

Since then it has been emphazised for quite some time [4,5] that these leading-lns calculations in the Higgs model are only the beginning of a whole reggeon field theory, and that all its elements are, in principle, determined by the general analytic structure of multiparticle amplitudes. This reggeon field theory then provides a unitary high energy description, with unitarity both for the direct channel and for the t-channel. Moreover, if the finiteness of the zero mass limit remains valid beyond the leading-lns approximation, one also obtains a high energy theory of QCD which, at least on the gluon level, is unitary. With such a highly constrained set of perturbative terms of QCD at hand, one might speculate that the transition into the nonperturbative regime is rather smooth. It is the goal of the present and a subsequent paper to continue the program of I and II beyond the leading lns approximation. More specifically, we attempt to construct the elements of the reggeon field theory explicitly, study their unitarity content and prepare the ground for a systematic study of the zero mass limit.

There are several reasons why the continuation of this rather long and tedious program may be of interest. First, there is still the annoying fact that, in hadron colliders, the majority of events cannot be described within QCD: the whole diffractive sector. The problem of low-p_T scattering in QCD is still waiting for a solution. This shortage becomes acute also with the deep inelastic structure functions moving towards smaller and smaller values of Bjorken-x: extending the presently known kinematic region into the small-x regime, the well-tested Altarelli-Parisi evolution equations [6,7,8] loose their validity. Moving, at fixed Q^2, to smaller and smaller values of x, one first probes a transition region, for which Gribov, Levin, and Ryskin [9] have suggested a modified evolution equation. But then one enters the nonperturbative regime which is the large-Q^2 extension of the Regge limit and is expected to be governed by the same dynamics. At not too large values of Q^2 (e.g. $Q^2 = 10GeV^2$ which will be relevant for HERA [4]), first estimates indicate that, in fact, we are very close to this nonperturbative regime. It is therefore clear that a better understanding of this limit will be of enormous help in analysing the small-x part of deep inelastic scattering. In fact, it is urgently needed.

Another motivation comes from the renewed interest in the high energy limit of W-W scattering in the standard electroweak model. A few years ago [11] it has been argued that certain pieces of the nonperturbative (topological nontrivial) sector lead to a very strongly rising total cross section for W-W scattering. Although more recent calculations [12,13,14] indicate that the growth of the production cross section is not as strong as originally expected, the question of the high energy behavior of, e.g. WW scattering, is not yet resolved: unless the Higgs mass is very large, the perturbative corrections to the Born scattering amplitude remain small up to rather large energies. But since the Regge limit will necessarily involve nonperturbative contributions, a more careful study even of the vicinity of the trivial vacuum is certainly needed. This provides a strong motivation for calculating the high energy behavior of the SU(2) Higgs model. The start of such an analysis is clearly the same as that of the above program: one has to isolate those terms of

the perturbation theory which are required by unitarity. The next step then deviates from the QCD-aimed approach: rather than being confronted with the difficulties of the theory at small momenta (long distances), one now faces the necessity to extend the perturbative analysis into the unknown ultraviolet part of the theory. Again, there is the hope that the perturbative analysis, satisfying so many unitarity constraints, will provide some clue of the ultraviolet extension of the theory.

All these reasons seem sufficiently strong to reenter and complete the old program started in I and II. We work again in the SU(2) Higgs model (for simplicity, we shall use "isospin" rather than "color"), and we shall make extensive use of results which have been obtained in these two papers. To make the reading somewhat simpler we first shall review some of the previous results on the leading-lns approximation. The first step beyond then involves the calculation of double energy discontinuities which lead to new elements: two-particle $\rightarrow$ three reggeon vertexfunctions (section II). After the decomposition of the group structure and the introduction of signature, these functions are shown to satisfy "bootstrap" equations, being new manifestations of the reggeization of the vector particle. With these elements we are able to construct new contributions to the partial waves (section III), in particular the three-reggeon cut. The next step are triple-energy discontinuities and two-particle $\rightarrow$ four-reggeon vertices (section IV). They contain, among other elements, also the leading contribution to the triple Pomeron vertex. After investigating the reggeization properties of these amplitudes, we show explicitly how production amplitudes with three-reggeon cuts and those with four reggeons satisfy both s-channel and t-channel unitarity: strictly speaking, unitarity is obtained only if we simultaneously fix both s and t channel discontinuities. The next section (section V) contains the attempt to generalize the results to the two-particle $\rightarrow$ n-reggeon vertex. We conclude with a brief summary. A few group theoretical details will be put into an appendix. The final step which will be presented in a subsequent paper consists of the construction of n-reggeon $\rightarrow$ m-reggeon vertex functions; diagrammatically, this leads to the "iteration in the t-channel"

of multireggeon intermediate states. Studies of the infrared limit as well as the connection with deep inelastic scattering in the small-x limit will also not be presented in this paper, but will be subjects of seperate publications.

2 Double Discontinuities and Three Reggeon Vertices

2.1 Review of previous results

Let us first recapitulate a few of the results of the leading-lns approximation in I. For the amplitude $T_{2\to n}$ the result is ([15,16,17,18,19] and I, eq.(4.75)) (Fig.1a):

$$T_{2\to n} = 2s[gH_{VV}]\frac{s_{12}^{\alpha_1-1}}{T_1}[g\Gamma(q_1,-q_2)]\frac{s_{23}^{\alpha_2-1}}{T_2}\cdots[g\Gamma(q_{n-2},-q_{n-1})]\frac{s_{n-1,n2}^{\alpha_{n-1}-1}}{T_{n-1}}[gH_{VV}]. \tag{2.1}$$

with

$$T_i = -q_i^2 - M^2 = t_i - M^2 \tag{2.2}$$

(here q_i denotes the two-dimensional transverse momentum). For the group structure we have (Fig.1b):

$$\epsilon_{a_1t_1b_1}\epsilon_{t_1t_2b_2}\epsilon_{t_2t_3b_3}\cdots\epsilon_{t_{n-1}a_2b_n}. \tag{2.3}$$

In (2.1), (2.3) all external particles are vector particles, and the vertex H_{VV} denotes a 3×3 matrix. Working in a Higgs model, we have to include also the Higgs scalar in all s-channel states, but in this paper we shall be not very explicit about its contribution (details are found in I). When evaluating energy discontinuities from unitarity integrals, results will always include the scalar particle. But when describing intermediate steps, we will restrict ourselves to the vector particles. This kind of simplifying our presentation may be justified by our ultimate main interest in the zero mass limit, where the whole Higgs sector is "frozen" out. We will allow ourselves even one further simplification: in all our formulas we will simply omit the matix H_{VV} (and the corresponding expression for the scalar) for the coupling of reggeons to external particles and only retain the coupling constant g. With the rules given in I it is fairly straightforward to restore this helicity dependence.

The result (2.1) was shown to be consistent with unitarity and single energy discontinuites. In order to discuss this in more detail it is necessary to use the Sommerfeld-Watson integral representations given in Table 1. For the case of $T_{2\to 2}$ the only discontinuity is that in the energy s. Unitarity requires that

$$disc_sT_{2\to 2} = \frac{1}{2}\sum_{n=2}^{\infty}\int d\Omega_nT_{2\to n}T^*_{2\to n} \tag{2.4}$$

(we always use the notation: $disc_sT(s) = \frac{1}{2i}(T(s+i\epsilon)-T(s-i\epsilon)$; $d\Omega$ denotes the n-particle phase space integral in the multiregge region). Inserting on the rhs the expressions from eq.(2.1) and taking the inverse Mellin transform with respect to the energy, one arrives at the reggeon diagrams shown in Fig.2a. Let $\omega = j-1$ (j=angular momentum) denote the reggeon energy, $t = -q^2$ the momentum transfer (q is the two-dimensional transverse momentum vector). By cutting off the particle vertex at the right end of the diagrams, one is lead to the definition of a two-particle → two-reggeon vertex function $D_2(k_1,k_2;\omega)$ which satisfies an integral equation (Fig.2b). The group structure is simplified by projecting on definite isospin in the t-channel (which is the same as decomposing all group tensors inside the diagrams into irreducible representations). Because of the pointlike structure of the particle-reggeon vertex, this decomposition of the group structure immediately leads to amplitudes with definite signature τ: $\tau = +$ for $I = 0$ or 2 and $\tau = -$ for $I = 1$. The integral equations for the signatured vertex functions $D_2^{(I;\tau)}$ are of the form:

$$\omega D_2^{(I;\tau)}(k_1,k_2) = -c^Ig^2 + D_2^{(I;\tau)}\otimes\left(c^IK_{2\to 2}(k_1,k_2)+\alpha(k_1)+\alpha(k_2)-2\right). \tag{2.5}$$

Here we have used a somewhat compact notation: the symbol "⊗" when used in connection with the kernel $K_{2\to 2}$, stands for the two dimensional integral

$$\int\frac{d^2k}{(2\pi)^3}. \tag{2.6}$$

In connection with the trajectory function $\alpha(k)$

$$\alpha(t) = 1 + (t - M^2)\beta_2(t)$$

$$\beta_2(t) = g^2 \int \frac{d^2k}{(2\pi)^3} \frac{1}{-k^2 - M^2} \frac{1}{-(k-q)^2 - M^2}$$
$$t = -k^2 \tag{2.7}$$

it means simple multiplication. Each (internal) reggeon line with momentum k carries the signature factor $\frac{1}{-k^2-M^2}$. Outgoing reggeon lines carry momenta k_1 and k_2, but momentum conservation requires, of course, that $k_1 + k_2 = q$ with $t = -q^2$. The kernel $K_{2\to 2}$ has the form

$$\frac{1}{g^2} K_{2\to 2}(k_1, k_2; k_1', k_2') = -(-q^2 - \frac{3}{2}M^2) + \frac{(-k_1^2 - M^2)(-k_2'^2 - M^2) + (-k_2^2 - M^2)(-k_1'^2 - M^2)}{-(k_1 - k_1')^2 - M^2} \tag{2.8}$$

(here the contribution of the intermediate scalar has not yet been included: it adds to the first term a constant proportional to M^2, but its weight depends upon the group decomposition. In particular, in the I=1 channel the first term in (2.8) turns into $-(-q^2 - M^2)$, which is crucial for the reggeization of the vector particle. As we have said above, when we state results they include the scalar, but we shall not explain in detail how they are obtained). Finally, the coefficients c^I in (2.5) are the results from the decomposition of the group structure: $c^I = -2, -1, 1$ for $I = 0, 1, 2$, resp.

As to the solutions of these equations, we remind that in the $I = 1$ odd-signature channel we have the famous "bootstrap" property ([16] and I, (5.7)) (Fig.2c):

$$D_2^{(1;-)} = g \frac{1}{\omega + 1 - \alpha(q)} g. \tag{2.9}$$

In the vacuum exchange channel, the leading j-plane singularity was found [15,20] to be a fixed-cut to the right of j=1; morover, in this channel the infrared singularities for $M^2 \to 0$ cancel.

It is also useful to define the "amputated" vertex functions $C_2^{(I;\tau)}$ which differ from the D's by the reggeon energy denominator of the external reggeon lines:

$$D_2^{(I;\tau)}(k_1, k_2; \omega) = C_2^{(I;\tau)}(k_1, k_2; \omega) \frac{1}{\omega + 2 - \alpha(k_1) - \alpha(k_2)}. \tag{2.10}$$

(to be precise, the D functions should then be called Green's functions or "nonamputated" vertex functions, but we shall not insist on this distinction). From (2.9) we obtain:

$$C_2^{(1;-)}(k_1, k_2; \omega) = g^2 \frac{\omega + 2 - \alpha(k_1) - \alpha(k_2)}{\omega + 1 - \alpha(q)}. \tag{2.11}$$

The numerator in this expression is a "cut killing" factor.

We now return to (2.4) and use (2.11) for the I=1 channel. Most naively, we could simply take $D_2^{(1;-)}$ and "close" the outgoing reggeon lines with the two-reggeon-two-particle vertex. With (2.9) and

$$disc_s T_{2\to 2}^{(1;-)} = -s \int \frac{dj}{2\pi i} s^{j-1} F(j,t) \tag{2.12}$$

we immediately find

$$F(j,t) = -2\pi g \frac{\beta_2(t)}{j - \alpha(t)} g \cdot P_1. \tag{2.13}$$

where P_1 denotes the projector defined in the appendix. For later purposes, however, it will be useful to repeat this calculation in a somewhat different way. Namely take the expression for the partial wave and do not yet invoke the bootstrap property (2.9). One then could try to take the discontinuity across the two reggeon cut. Near the tip of the cut we have (ignoring the group structure):

$$disc_\omega F(j,t) = -2\pi^2 \int \frac{d^2k}{(2\pi)^3} C_2^{(1;-)} \delta(\omega + 2 - \alpha(k) - \alpha(q-k)) \frac{1}{(-k^2 - M^2)(-(q-k)^2 - M^2)} C_2^{(1;-)}. \tag{2.14}$$

Using now (2.11), the "cut killing factors" in both residue functions C_2 remove the two reggeon cut singularity. Adopting the point of view that all expressions which we obtain in this dispersion relation-based approach have an unambigous meaning only near singularities in the t-channel (either particle or reggeon discontinuities), we have to move onto the two particle cut. With the observation that (2.7) can clearly be written as:

$$\beta_2(t) = \frac{1}{\pi} \int_{4M^2}^{\infty} dt' \frac{disc_t \beta_2(t')}{t' - t} \tag{2.15}$$

we interpret the partial wave (2.13) as the analytic continuation of a t-dispersion integral:

$$F(j,t) = \frac{1}{\pi} \int_{4M^2}^{\infty} \frac{dt'}{t' - t} g\, disc_t \left(\frac{-2\pi\beta_2(t')}{\omega + 1 - \alpha(t')} \right) g P_1. \tag{2.16}$$

This means that, strictly speaking, we first go to the physical region of the t-channel, calculate the two-particle cut for the dispersion integral, then continue to negative t-values. This determines the partial wave. Expanding the signature factor of $T_{2\to 2}$ in powers of g^2, one finds:

(i) the leading term is real and agrees with (2.1;

(ii) the next-to leading term (which is down by one power of g^2) is equal to $i \cdot disc_s$.

(iii) For the even signature channels the g^2 expansion starts, at the next-to-leading-lns level, with the imaginary discontinuity, and the real parts are down by one more power of g^2. So the sum of all next-to-leading terms are just the reggeon diagrams of Fig.2a. (multiplied by i). In the following discussion it will be useful to keep track of these powers of g^2 as a counting parameter.

All this was discussed in I and II. It was then also shown that the two-particle $\to$ two-reggeon-vertices can be used to construct the partial waves of the inelastic amplitudes $T_{2\to 3}$, $T_{2\to 4}$, and $T_{3\to 3}$ (Table 1). For the case $T_{2\to 3}$ single discontinuities in s_{ab} and s_{bc} obviously suffice to uniquely determine the two partial waves, and for $T_{2\to 4}$ one also has enough equations to fix the partial waves. In particular, for the leading real part of the amplitudes with odd signature in all t-channels, the various partial waves combine with the signature factors in table 1 just in the right way to reproduce the result eq.(2.1). In II we also considered amplitudes with even signature in some of the t-channels, which means one step beyond the leading -lns approximation.

2.2 Double discontinuitis and three-reggeon vertices

To proceed further requires some new ingredients. This starts from the observation that the previous construction of the inelastic amplitudes remains unsatisfactory: a clean determination of the partial waves requires multiple energy discontinuities. As an example, the $2 \to 3$ amplitude from table 1 splits into two pieces, each of which satisfies a double dispersion relation with subtraction integrals and subtraction constants. If s-channel unitarity

is used to determine the double discontinuities, there is no ambiguity due to real parts or subtractions. In Regge theory, all these terms are linked together through the signature factors, so one might use them to obtain real parts from the imaginary parts or vice versa. In I and II we used the latter method, when we evaluated single discontinuites only: for the inelastic amplitudes they represent subtraction integrals. Conceptually one might consider it preferable to go the other way: first calculate, from unitarity, multiple discontinuities which uniquely fix the partial waves. Of course, if one trusts that the SU(2) Higgs model obeys all the constraints that follow from Regge theory, there is no need to prefer one way to the other. Nevertheless, as we shall demonstrate on this paper, multiple discontinuities turn out to be inevitable: they lead to the definition of two-particle $\to$ n-reggeon vertices, and more general, n-reggeon $\to$ m-reggeon vertices. These vertices can then be used to construct, by invoking reggeon unitarity in the t-channel, $2 \to 2$ amplitudes with more than two reggeons in the t-channel and so on. This is, in short, the program of this paper.

Let us then turn to the amplitude $T_{2\to 3}$ and consider the two double-discontinuities $disc_s disc_{s_{ab}}$ and $disc_s disc_{s_{bc}}$. It will be useful to use the diagrammatic notation, introduced in Figs.1a and b. Unitarity then leads to the results shown in Figs.3a and b. Note that at this stage the group structure has not yet been reduced, i.e.each vertex is associated with an ϵ-tensor (or products of ϵ tensors). In order to analyse these double discontinuities it is useful to define two-particle $\to$ three-reggeon vertex functions $C_3(q-k_2-k_3, k_2, k_3; \omega, \omega_{23})$. (Fig.3c). The ω variables denote the reggeon energies in the (123) system and in the (23) subsystem, respectively. These energies are independent variables ("energy nonconserving vertex"). We also need a modified version $C_3(q-k_2-k_3, k_2, k_3; \omega)$, which differs from the previous one in that it has only one energy variable ("energy conserving vertex"). These functions C are defined in such a way that they do not include reggeon propagators for the external reggeon lines ("amputated" vertex functions). For the energy conserving vertex, it is useful to define also the analogous "nonamputated" vertex function (or Green's functions) $D_3(q-k_2-k_3, k_2, k_3; \omega)$ which differs from C by the energy denominator $1/(\omega -$

$\alpha(q-k_2-k_3)-\alpha(k_2)-\alpha(k_3)+3)$ for the external reggeon lines. In group space, all these functions are tensors with five indices. For the energy-conserving vertex we have an integral equation which is illustrated in Fig.3c (the expressions for the interaction vertices will be given below).

Before we can search for solutions, it is necessary to decompose the group tensors into irreducible representations and to introduce signature. The latter requires to define the order in which angular momenta are coupled together: we choose the scheme of Fig.4a (this corresponds to the "hexagraphs" of [3]), i.e. first the angular momenta of line "2" and "3" are coupled together, then the sum is combined with line "1". In accordance with this scheme, we search for irreducible representations in the (23) subsystem ($I_{23}=0,1,2$), then in the system formed by (23) and reggeon "1". This SU(2) decomposition requires a little algebra which we defer to the appendix: we define normalized tensors $T_{I,I_{23}}$ with definite isospin content (I,I_{23}) and decompose the tensors C into products $C^{(I,I_{23})}\cdot T_{I,I_{23}}$, where the $C^{(I,I_{23})}$ are scalar functions. The same applies to the amputated vertex functions C. This leads to a set of coupled integral equations of the different $C^{I,I_{23}}$'s. . Finally, we need to define signatured amplitudes: symmetrization or antisymmetrization in the momenta k_2 and k_3, then symmetrization or antisymmetrization in the particles at the left side of the vertex. Signature is then defined as parity under the *combined* exchange of momenta and group indices.

We are now ready to write down the integral equations for the signatured vertex functions $D_3^{(I,I_{23};\tau,\tau_{23})}$: their graphical illustration is still that of Fig.3, but all the group structure is now taken out from the diagrams, and the momenta in the (23)-subsystem are symmetrized or antisymmetrized. We begin with the channel $I=0$. The only group

tensor is T_{01}, and for the two amplitudes we find:

$$\begin{aligned}
&\omega D_3^{(01;+-)}(k_1,k_2,k_3;\omega)=\sqrt{2}g^3+\sqrt{2}D_2^{(0;+)}\otimes K_{2\to3}(k_1\{k_2k_3\})\\
&+D_3^{(01;+-)}\otimes[-K_{2\to2}(k_2k_3)+\alpha(k_1)+\alpha(k_2)+\alpha(k_3)-3-K_{2\to2}(k_1k_2)-K_{2\to2}(k_1k_3)]\\
&\omega D_3^{(01;++)}(k_1,k_2,k_3;\omega)=+\sqrt{2}D_2^{(0;+)}\otimes K_{2\to3}(k_1[k_2k_3])\\
&+D_3^{(01;++)}\otimes[-K_{2\to2}(k_2k_3)+\alpha(k_1)+\alpha(k_2)+\alpha(k_3)-3-K_{2\to2}(k_1k_2)-K_{2\to2}(k_1k_3)].
\end{aligned}\tag{2.17}$$

Here (II,(A.17)):

$$\begin{aligned}
\frac{1}{g^3}K_{2\to3}(k_1k_2;k_1'k_2'k_3')=&+(-q^2-\frac{7}{4}M^2)\\
&-\frac{(-(k_1'+k_2')^2-\frac{3}{2}M^2)(-k_2^2-M^2)}{-(k_2-k_3')^2-M^2}-\frac{(-(k_2'+k_3')^2-\frac{3}{2}M^2)(-k_1^2-M^2)}{-(k_1-k_1')^2-M^2}\\
&+\frac{(-k_1^2-M^2)(-k_2^2-M^2)(-k_2'^2-M^2)}{(-(k_1-k_1')^2-M^2)(-(k_2-k_3')^2-M^2)},
\end{aligned}\tag{2.18}$$

and $\{...\}$, $[...]$ means symmetrization and antisymmetrization in the momentum variables, resp. (scalars are not yet included). These equations can be solved partially: the D_3 vertex functions can be reduced to the D_2 functions, namely (Fig.5):

$$\begin{aligned}
D_3^{(01;+-)}(k_1,k_2,k_3) &= \frac{1}{\sqrt{2}}D_2^{(0;+)}(k_1,k_2+k_3;\omega)\cdot g\\
D_3^{(01;++)}(k_1,k_2,k_3) &= \frac{1}{\sqrt{2}}\left(D_2^{(0;+)}(k_1+k_2,k_3;\omega)-D_2^{(0;+)}(k_1+k_3,k_2;\omega)\right)\cdot g.
\end{aligned}\tag{2.19}$$

The first of these two equations is of the familiar form (2.9): two adjacent reggeon lines, being in a $(I=1,\tau=-)$ state, "collapse" into one reggeon. The second equation is of a new type. We shall come back to this somewhat later.

Next we come to the case $I=1$. Group tensors are T_{10}, T_{11}, and T_{12}. We have two sets of coupled integral equations:

$$\begin{aligned}
&\omega D_3^{(11;--)}(k_1,k_2,k_3;\omega)=\tfrac{1}{\sqrt{2}}g^3+\tfrac{1}{\sqrt{2}}D_2^{(1;-)}\otimes K_{2\to3}(k_1\{k_2k_3\})\\
&+D_3^{(11;--)}\otimes[-K_{2\to2}(k_2k_3)+\alpha(k_1)+\alpha(k_2)+\alpha(k_3)-3-\tfrac{1}{2}K_{2\to2}(k_1k_2)-\tfrac{1}{2}K_{2\to2}(k_1k_3)]\\
&+D_3^{(10;--)}\otimes[\tfrac{2}{\sqrt{3}}K_{2\to2}(k_1,k_2)-\tfrac{2}{\sqrt{3}}K_{2\to2}(k_1,k_3)]\\
&+D_3^{(12;--)}\otimes[\sqrt{\tfrac{5}{12}}K_{2\to2}(k_1,k_2)-\sqrt{\tfrac{5}{12}}K_{2\to2}(k_1,k_3)],
\end{aligned}\tag{2.20}$$

$$\omega D_3^{(10;--)}(k_1,k_2,k_3;\omega) = -\sqrt{\tfrac{8}{3}} D_2^{(1;-)} \otimes K_{2\to 3}(k_1[k_2k_3])$$
$$+D_3^{(10;--)} \otimes [-2K_{2\to 2}(k_2k_3) + \alpha(k_1) + \alpha(k_2) + \alpha(k_3) - 3]$$
$$+D_3^{(11;--)} \otimes [\tfrac{2}{\sqrt{3}} K_{2\to 2}(k_1,k_2) - \tfrac{2}{\sqrt{3}} K_{2\to 2}(k_1,k_3)], \tag{2.21}$$

$$\omega D_3^{(12;--)}(k_1,k_2,k_3;\omega) = -\sqrt{\tfrac{5}{6}} D_2^{(1;-)} \otimes K_{2\to 3}(k_1[k_2k_3])$$
$$+D_3^{(12;--)} \otimes [K_{2\to 2}(k_2k_3) + \alpha(k_1) + \alpha(k_2) + \alpha(k_3) - 3 - \tfrac{3}{2} K_{2\to 2}(k_1,k_2) - \tfrac{3}{2} K_{2\to 2}(k_1,k_3)]$$
$$+D_3^{(11;--)} \otimes [\sqrt{\tfrac{5}{12}} K_{2\to 2}(k_1,k_2) - \sqrt{\tfrac{5}{12}} K_{2\to 2}(k_1,k_3)]. \tag{2.22}$$

For the second set we find:

$$\omega D_3^{(11;-+)}(k_1,k_2,k_3;\omega) = +\tfrac{1}{\sqrt{2}} D_2^{(1;-)} \otimes K_{2\to 3}(k_1[k_2k_3])$$
$$+D_3^{(11;-+)} \otimes [-K_{2\to 2}(k_2k_3) + \alpha(k_1) + \alpha(k_2) + \alpha(k_3) - 3 - \tfrac{1}{2} K_{2\to 2}(k_1k_2) - \tfrac{1}{2} K_{2\to 2}(k_1k_3)]$$
$$+D_3^{(10;-+)} \otimes [\tfrac{2}{\sqrt{3}} K_{2\to 2}(k_1,k_2) - \tfrac{2}{\sqrt{3}} K_{2\to 2}(k_1,k_3)],$$
$$+D_3^{(12;-+)} \otimes [\sqrt{\tfrac{5}{12}} K_{2\to 2}(k_1,k_2) - \sqrt{\tfrac{5}{12}} K_{2\to 2}(k_1,k_3)], \tag{2.23}$$

$$\omega D_3^{(10;-+)}(k_1,k_2,k_3;\omega) = -\sqrt{\tfrac{8}{3}} g^3 - \sqrt{\tfrac{8}{3}} D_2^{(1;-)} \otimes K_{2\to 3}(k_1\{k_2k_3\}$$
$$+D_3^{(10;-+)} \otimes [-2K_{2\to 2}(k_2k_3) + \alpha(k_1) + \alpha(k_2) + \alpha(k_3) - 3] \tag{2.24}$$
$$+D_3^{(11;-+)} \otimes [\tfrac{2}{\sqrt{3}} K_{2\to 2}(k_1,k_2) - \tfrac{2}{\sqrt{3}} K_{2\to 2}(k_1,k_3)],$$

and

$$\omega D_3^{(12;-+)}(k_1,k_2,k_3;\omega) = -\sqrt{\tfrac{5}{6}} g^3 - \sqrt{\tfrac{5}{6}} D_2^{(1;-)} \otimes K_{2\to 3}(k_1\{k_2k_3\})$$
$$+D_3^{(12;-+)} \otimes [K_{2\to 2}(k_2k_3) + \alpha(k_1) + \alpha(k_2) + \alpha(k_3) - 3 - \tfrac{3}{2} K_{2\to 2}(k_1,k_2) - \tfrac{3}{2} K_{2\to 2}(k_1,k_3)]$$
$$+D_3^{(11;-+)} \otimes [\sqrt{\tfrac{5}{12}} K_{2\to 2}(k_1,k_2) - \sqrt{\tfrac{5}{12}} K_{2\to 2}(k_1,k_3)]. \tag{2.25}$$

For the first set the solutions are:

$$D_3^{(11;--)}(k_1,k_2,k_3;\omega) = \frac{1}{\sqrt{2}} D_2^{(1;-)}(k_1,k_2+k_3;\omega)\cdot g$$
$$= \frac{g}{\sqrt{2}} \frac{1}{\omega + 1 - \alpha(k_1+k_2+k_3)} \cdot g^2 \tag{2.26}$$

and

$$D_3^{(10;--)}(k_1,k_2,k_3;\omega) = 0$$
$$D_3^{(12;--)}(k_1,k_2,k_3;\omega) = 0. \tag{2.27}$$

For the second (even-signature) set there is no "contraction" of two reggeon lines in the final state. The only simplification occurs in the two-reggeon intermediate state in the left part of the diagrams (Fig.6): this leads to the new one-reggeon $\to$ three reggeon vertex. The analytic form can easily be obtained from (2.11) and (2.18), and we do not give the result here.

Finally the case $I = 2$. The relevant tensors are T_{21}, T_{22}. The equations come in two pairs of coupled equations:

$$\omega D_3^{(21;+-)}(k_1,k_2,k_3;\omega) = -\tfrac{1}{\sqrt{2}} g^3 - \tfrac{1}{\sqrt{2}} D_2^{(2;+)} \otimes K_{2\to 3}(k_1\{k_2k_3\})$$
$$+D_3^{(21;+-)} \otimes [-K_{2\to 2}(k_2k_3) + \alpha(k_1) + \alpha(k_2) + \alpha(k_3) - 3 + \tfrac{1}{2} K_{2\to 2}(k_1k_2) + \tfrac{1}{2} K_{2\to 2}(k_1k_3)]$$
$$+D_3^{(22;+-)} \otimes [\tfrac{\sqrt{3}}{2} K_{2\to 2}(k_1,k_2) - \tfrac{\sqrt{3}}{2} K_{2\to 2}(k_1,k_3)], \tag{2.28}$$

$$\omega D_3^{(22;+-)}(k_1,k_2,k_3;\omega) = -\sqrt{\tfrac{3}{2}} D_2^{(2;+)} \otimes K_{2\to 3}(k_1[k_2k_3])$$
$$+D_3^{(22;+-)} \otimes [K_{2\to 2}(k_2k_3) + \alpha(k_1) + \alpha(k_2) + \alpha(k_3) - 3 - \tfrac{1}{2} K_{2\to 2}(k_1k_2) - \tfrac{1}{2} K_{2\to 2}(k_1k_3)]$$
$$+D_3^{(21;+-)} \otimes [\tfrac{\sqrt{3}}{2} K_{2\to 2}(k_1,k_2) - \tfrac{\sqrt{3}}{2} K_{2\to 2}(k_1,k_3)], \tag{2.29}$$

and

$$\omega D_3^{(21;++)}(k_1,k_2,k_3;\omega) = -\tfrac{1}{\sqrt{2}} D_2^{(2;+)} \otimes K_{2\to 3}(k_1|k_2k_3])$$

$$+D_3^{(21;++)} \otimes [-K_{2\to 2}(k_2k_3) + \alpha(k_1) + \alpha(k_2) + \alpha(k_3) - 3 + \tfrac{1}{2}K_{2\to 2}(k_1k_2) + \tfrac{1}{2}K_{2\to 2}(k_1k_3)]$$

$$+D_3^{(22;++)} \otimes [\tfrac{\sqrt{3}}{2}K_{2\to 2}(k_1,k_2) - \tfrac{\sqrt{3}}{2}K_{2\to 2}(k_1,k_3)], \tag{2.30}$$

$$\omega D_3^{(22;++)}(k_1,k_2,k_3;\omega) = -\sqrt{\tfrac{3}{2}}g^3 - \sqrt{\tfrac{3}{2}} D_2^{(2;+)} \otimes K_{2\to 3}(k_1\{k_2k_3\})$$

$$+D_3^{(22;++)} \otimes [K_{2\to 2}(k_2k_3) + \alpha(k_1) + \alpha(k_2) + \alpha(k_3) - 3 - \tfrac{1}{2}K_{2\to 2}(k_1k_2) - \tfrac{1}{2}K_{2\to 2}(k_1k_3)]$$

$$+D_3^{(21;++)} \otimes [\tfrac{\sqrt{3}}{2}K_{2\to 2}(k_1,k_2) - \tfrac{\sqrt{3}}{2}K_{2\to 2}(k_1,k_3)]. \tag{2.31}$$

Solutions to first two equations are:

$$D_3^{(21;+-)}(k_1,k_2,k_3;\omega) = \frac{1}{\sqrt{2}} D_2^{(2;+)}(k_1,k_2+k_3;\omega)\cdot g \tag{2.32}$$

and

$$D_3^{(22;+-)}(k_1,k_2,k_3;\omega) = 0. \tag{2.33}$$

For the other two equations one finds:

$$D_3^{(22;++)}(k_1,k_2,k_3;\omega) = \frac{1}{2}\sqrt{\frac{3}{2}}\left(D_2^{(2;+)}(k_1+k_2,k_3;\omega) + D_2^{(2;+)}(k_1+k_3,k_2;\omega)\right)\cdot g \tag{2.34}$$

and

$$D_3^{(21;++)}(k_1,k_2,k_3;\omega) = -\frac{1}{2\sqrt{2}}\left(D_2^{(2;+)}(k_1+k_2,k_3;\omega) - D_2^{(2;+)}(k_1+k_3,k_2;\omega)\right)\cdot g. \tag{2.35}$$

These two equations, together with the second solution in (2.19), represent a new type of "bootstrap" equation: reggeon "1" forms, together with the pair "2" and "3" which are in a positive signature state, another positive signature state. In order to avoid violation of signature conservation, the three-reggeon cut must cancel.

In order to discuss multiple energy discontinuities in production amplitudes we still need one further generalization, namely multireggeon vertices with two independent reggeon

energies. The diagrammatic rules for such reggeon diagrams have been derived long time ago [21,22], and they are quite simple. In a typical diagram (Fig.7), when passing from the left end to the right end, there is one "last" interaction, before the two branches separate. Denote this last interaction vertex by "branching vertex". To the left of this vertex, the sum of reggeon energies equals ω, to the right each branch has its own total energy, say ω' and ω''. There is no conservation law which forces $\omega = \omega' + \omega''$. In our case, one of the branches (ω') consists of one reggeon line which, at $t' = M^2$, becomes a particle; the left energy variable is ω_1, and ω'' is identified with ω_2. With these rules, it is not difficult to generalize the integral equations of Fig.3c (for the time being, we stay away from $t' = M^2$) to the energy nonconserving situation (Fig.7b). To the left of the branching vertex, we have the vertex functions D_3 which have been discussed before. They depend upon the one energy variable ω_1. Then comes the branching vertex: reggeon "1" can be attached either to line "2" or "3", or to the "connected" interaction vertex two-reggeons $\to$ three reggeons. Further to the right, all energy denominators depend upon ω_2, and we have to sum over the pairwise interactions in the (23)-subsystem.

To illustrate the structure of the integral equations, we write down the equation for two typical cases. First the channel $(11;--)$:

$$C_3^{(11;--)}(k_1,k_2,k_3;\omega_1,\omega_2) = \tfrac{1}{\sqrt{2}} D_2^{(1;-)} \otimes K_{2\to 3}(k_1\{k_2k_3\})$$

$$+D_3^{(11;--)}(k_1,k_2,k_3;\omega_1) \otimes [-\tfrac{1}{2}K_{2\to 2}(k_1,k_2) - \tfrac{1}{2}K_{2\to 2}(k_1,k_3)] \tag{2.36}$$

$$-C_3^{(11;--)}(k_1,k_2,k_3;\omega_1,\omega_2) \otimes \tfrac{1}{\omega_2+2-\alpha(k_2)-\alpha(k_3)} K_{2\to 2}(k_2,k_3)$$

(we have left out two terms which vanish due to (2.27)). It has the solution (Fig.7c):

$$C_3^{(11;--)}(k_1,k_2,k_3;\omega_1,\omega_2) = -\frac{1}{\sqrt{2}} D_2^{(1;-)} \otimes K_{2\to 2}(k_1,k_2+k_3)$$
$$\cdot\frac{\omega_2+2-\alpha(k_2)-\alpha(k_3)}{\omega_2+1-\alpha(k_2+k_3)}\cdot g. \tag{2.37}$$

The second case is the channel $(22;++)$. The integral equation reads:

$$
\begin{aligned}
C_3^{(22;++)}(k_1,k_2,k_3;\omega_1,\omega_2) &= -\sqrt{\tfrac{3}{2}}D_2^{(2;+)}\otimes K_{2\to 3}(k_1\{k_2k_3\}) \\
&+D_3^{(22;++)}(k_1,k_2,k_3;\omega_1)\otimes[-\tfrac{1}{2}K_{2\to 2}(k_1,k_2)-\tfrac{1}{2}K_{2\to 2}(k_1,k_3)] \\
&+D_3^{(21;++)}(k_1,k_2,k_3;\omega_1)\otimes[\tfrac{\sqrt{3}}{2}K_{2\to 2}(k_1,k_2)-\tfrac{\sqrt{3}}{2}K_{2\to 2}(k_1,k_3)] \\
&+C_3^{(22;++)}(k_1,k_2,k_3;\omega_1,\omega_2)\otimes\tfrac{1}{\omega_2+2-\alpha(k_2)-\alpha(k_3)}K_{2\to 2}(k_2,k_3).
\end{aligned}
\tag{2.38}
$$

Its formal solution is:

$$
\begin{aligned}
C_3^{(22;++)}(k_1,k_2,k_3;\omega_1,\omega_2) &= \Bigg(\sqrt{\frac{3}{2}}D_2^{(2;+)}\otimes K_{2\to 3}(k_1\{k_2k_3\}) \\
&+D_3^{(22;++)}(k_1,k_2,k_3;\omega_1)\otimes[-\frac{1}{2}K_{2\to 2}(k_1,k_2)-\frac{1}{2}K_{2\to 2}(k_1,k_3)] \\
&+D_3^{(21;++)}(k_1,k_2,k_3;\omega_1)\otimes[\frac{\sqrt{3}}{2}K_{2\to 2}(k_1,k_2)-\frac{\sqrt{3}}{2}K_{2\to 2}(k_1,k_3)]\Bigg) \\
&\otimes G_{2\to 2}^{(2;+)}(k_2,k_3;\omega_2)(\omega_2+2-\alpha(k_2)-\alpha(k_3)),
\end{aligned}
\tag{2.39}
$$

where $G_{2\to 2}^{(2;+)}$ is the Green's function for the two- reggeons $\to$ two-reggeons amplitude in the $I=2,\tau=+$ channel:

$$
\begin{aligned}
G_{2\to 2}^{(2;+)}(k_1,k_2;\omega) &= \tfrac{1}{\omega+2-\alpha(k_1)-\alpha(k_2)} \\
&+G_{2\to 2}^{(2;+)}\otimes K_{2\to 2}(k_1,k_2)\tfrac{1}{\omega+2-\alpha(k_1)-\alpha(k_2)}.
\end{aligned}
\tag{2.40}
$$

For the second and third lines in (2.39) we use (2.34) and (2.35). The result is:

$$
\begin{aligned}
&-\frac{1}{2}\sqrt{\frac{3}{2}}\Big(D_2^{(2;+)}(k_1+k_2,k_3;\omega_1)\otimes K_{2\to 2}(k_1,k_2) \\
&\quad +D_2^{(2;+)}(k_1+k_3,k_2;\omega_1)\otimes K_{2\to 2}(k_1,k_3)\Big)\cdot g.
\end{aligned}
\tag{2.41}
$$

With the property

$$
\begin{aligned}
&D_2^{(2;+)}(k_1+k_2,k_3;\omega_1)\otimes K_{2\to 2}(k_1,k_2) = \\
&\quad -D_2^{(2;+)}(k_1+k_2,k_3;\omega_1)\cdot(\alpha(k_1+k_2)+1-\alpha(k_1)-\alpha(k_2))
\end{aligned}
\tag{2.42}
$$

and a few algebraic manipulations the solution (2.39) can be rewritten (Fig.7d):

$$
C_3^{(22;++)}(k_1,k_2,k_3;\omega_1,\omega_2) =
$$

$$
\begin{aligned}
&\frac{1}{2}\sqrt{\frac{3}{2}}\Bigg(C_2^{(2;+)}(\omega_1)\otimes\frac{g(\omega_1-\omega_2-\alpha(k_1)+1)}{\omega_1+2-\alpha(k_1)-\alpha(k_2)}G_{2\to 2}(k_2,k_3;\omega_2)\cdot(\omega_2+2-\alpha(k_2)-\alpha(k_3)) \\
&\qquad +C_2^{(2;+)}(\omega_1)\otimes\frac{g(\omega_2+2-\alpha(k_2)-\alpha(k_3))}{\omega_1+2-\alpha(k_1)-\alpha(k_2)}\Bigg) \\
&\qquad +(k_2\leftrightarrow k_3).
\end{aligned}
\tag{2.43}
$$

A very similar discussion applies to other configurations of the t_{23} channel, such as $(10;-+)$, $(12;-+)$, $(21;+-)$. This completes our discussion of three reggeon vertices.

2.3 The $T_{2\to 3}$ amplitude

With the results of the previous subsection we now return to the amplitude $T_{2\to 3}$ and demonstrate that the double discontinuities lead to the same partial waves F_1 and F_2 as those obtained in I and II from the single discontinuities. It also allows to determine nonleading pieces of $T_{2\to 3}$ which we shall need later on.

First we use our energy nonconserving amplitudes $C_3^{(I,I_{23};\tau,\tau_{23})}$ in order to find the partial waves: this is most easily done by going taking all three $k_i^2=M^2$. Subsequently, we replace in the t_2-channel the last four reggeon vertex by the particle coupling g^2, and on the line of reggeon "1" we put the production vertex Γ from (I,(3.6)). All this can be done either at the initial expressions for the C's, i.e before any contraction of neighbored reggeon lines is invoked, or in the solutions to the integral equations. It is useful to have both versions at hand.

Now one has to consider each (isospin, signature) case seperately. Rather than going through this in all detail, we only mention a few major points, which can all be verified rather easily.

The first point is the fact that all partial waves coincide with those of I and II, except for $F_i^{(22;++)}$ (i=1,2), $F_1^{(21;+-)}$ and $F_2^{(12;-+)}$ which did not appear at that level of accuracy. From this it follows, in particular, that the leading real part of the odd signature amplitude (2.1) is consistent with both double and single discontinuities. As to the first two partial waves, $F_i^{(22;++)}$ (i=1,2), the calculations based on single energy discontinuities lead only

to a combination of these two partial waves and signature factors, but did not allow to determine the partial waves seperately. It therefore remains to demonstrate that the results from the present analysis, when combined in the suitable way, are consistent with the results from II.

To this end, we start from (2.39). This expression describes the two- particle → three-reggeon vertex. In order to find the partial wave $F_2^{(22;++)}$ a few modifications are needed. First, we have to change reggeon "1" into a particle: we have to go on the reggeon energy mass shell ($\omega_1 = \alpha(k_1) - 1$) and to the four- momentum mass shell ($-k_1^2 = M^2$). As an example, we mention that the kernel $K_{2\to 2}$ in (2.39) has to be replaced by (cf.(2.8)):

$$g^2\Gamma(k_1 + k_2, k_2') - g^2\Gamma(k_1, k_1 - k_1')\frac{-k_2'^2 - M^2}{-(k_1 - k_1')^2 - M^2}, \tag{2.44}$$

where Γ is the production vertex from (I,(3.6)). Correspondingly, the rhs of (2.42) has to be replaced by:

$$D_2^{(2;+)}(k_1 + k_2, k_3; \omega_1) \cdot (\alpha(k_1 + k_2) - 1 - K(k_1, -k_2)), \tag{2.45}$$

where (cf.I.(4.45)):

$$K(k_1, -k_2) = g^2 \int \frac{d^2k}{(2\pi)^3} \frac{1}{-k^2 - M^2} \frac{1}{-(k_1 - k)^2 - M^2} \frac{1}{-(k_2 - k)^2 - M^2} \cdot \Gamma(k_1 - k, -k_2 + k). \tag{2.46}$$

Secondly, also reggeons "2" and "3" become particles. This is achieved by either taking these lines on energy and mass shell, as demonstrated for line "1", and changing the definition of $G_{2\to 2}$ in (2.40) in such a way that it contains at least one kernel $K_{2\to 2}$. More simply, we can close the outgoing lines "2" and "3" with a pointlike two-reggeon → two-particle vertex g^2. The final result for the partial wave is:

$$F_2^{(22;++)} = -\pi^2\sqrt{\frac{3}{2}} \int \frac{d^2k}{(2\pi)^3} D_2^{(2;+)}(k_1 + k, k; \omega_1) \frac{1}{-k^2 - M^2} \frac{1}{-(k_1 + k)^2 - M^2} \frac{1}{-(k_2 + k)^2 - M^2} \cdot g\Gamma(k_1 + k, -k_2 - k)[(\omega_1 - \omega_2 + \alpha(k_2) + K(k_1 + k, -k_2 - k))\, D_2^{(2;+)}(k_2 + k, k; \omega_2)]. \tag{2.47}$$

(this result is still to be multiplied by the group tensor T_{22}). A similar result is derived for $F_1^{(22;++)}$.

With these results we go into the representation of Table 1 and expand the signature factors, retaining only the leading order. Observing certain cancellations between the denominators $\omega_1 - \omega_2$ and similar terms in the numerators, the two terms of $T_{2\to 3}$ combine, and the Mellin transform of $disc_s T_{2\to 3}$ (denoted by $F^{(22;++)}$) near the two-reggeon cut singularities in the t-channels takes the form:

$$F^{(22;++)} = -2\pi\sqrt{\frac{3}{2}} \int \frac{d^2k}{(2\pi)^3} D_2^{(2;+)}(k_1 + k, k; \omega_1') \frac{1}{-k^2 - M^2} \frac{1}{-(k_1 + k)^2 - M^2} \cdot g\Gamma(k_1 + k, -k_2 - k) \frac{1}{-(k_2 + k)^2 - M^2} D_2^{(2;+)}(k_2 + k, k; \omega_2) \tag{2.48}$$

(with the group structure T_{22}). This agrees with the result of I and II, which was obtained from the single discontinuity in s.

The other result which goes beyond that of II is the form of $F_1^{(21;+-)}$ (and, by symmetry that for $F_2^{(12;-+)}$), as shown in Fig.8a. It contains the three reggeon cut, and the reason why it did not appear in II is the simple fact that this signature configuration does not belong to the next-to-leading-lns approximation but one further step below. The appearance of this new partial wave which could not have been obtained from the methods of I and II is, in a certain sense, the main result of this section II. In the following section this three reggeon amplitude will allows us to construct new real parts for $T_{2\to 2}$.

Once we have verified that double and single energy discontinuities and real parts are consistent we can trust our results down to two steps beyond leading order (i.e.the order of the double discontinuities). In other words, we are allowed to expand the products of signature factors in Table 1 up to the order $O(g^0)$. Listing our results in ascending order of powers of g^2, we have:

0) Leading-lns approximation: here only the configuration with odd signature in both t-channels contributes, and the amplitude has the form (2.1).

1) Next-to leading order: single energy discontinuities in some of the signature configurations (the disconinuity in s_{ab} for (+,-) and (-,-), the discontinuity in s_{bc} for (-,+) and (-,-), and the s-discontinuity for all (-,-) and (+,+)).

2) Next-next-to-leading order: double discontinuities in all signature combinations. Diagrammatically, these contributions can be described as the sum of reggeon diagrams with up to three reggeon lines in the t-channels.

There is still another contribution to the (-,-) configuration which has not been mentioned so far. Our results for F_1 and F_2 (we supress the superscripts for group and signature) are:

$$\frac{2}{\pi^2}F_1 = g\frac{1}{\omega_1+1-\alpha(q_1)}[\omega_1\omega_2 g\Gamma - \omega_1 g K(q_1,-q_2)]\frac{1}{\omega_2+1-\alpha(q_2)}g \tag{2.49}$$

and

$$\frac{2}{\pi^2}F_2 = g\frac{1}{\omega_1+1-\alpha(q_1)}[\omega_1\omega_2 g\Gamma - \omega_2 g K(q_1,-q_2)]\frac{1}{\omega_2+1-\alpha(q_2)}g. \tag{2.50}$$

with the group structure analogous to Fig.1b. With this we go into the representation of Table 1. For the energy factors we write:

$$\begin{aligned} s^{j_1}s_{bc}^{j_2-j_1} &= s s_{ab}^{\omega_1} s_{bc}^{\omega_2}\eta^{-\omega_1} \\ \eta &= (q_1-q_2)^2+M^2. \end{aligned} \tag{2.51}$$

Expanding the signature factors in powers of g^2 we find a nonleading real-valued contribution to $T_{2\to3}$ of the same form as (2.1), but with the production vertex $g\Gamma$ being replaced by

$$g^2 K(q_1,-q_2)ln\eta. \tag{2.52}$$

We interpret this as a "cut" production vertex (Fig.8b).

3 New Real Parts for $T_{2\to2}$ and $T_{n\to m}$

One of the results of the previous section was the definition of the two-particle $\to$ three-reggeon vertices $D_3^{(1I_{23};--)}$ (which, in particular, contains the new $1\to3$ reggeon vertex). We now use this vertex to construct new pieces in $T_{2\to2}$. From Regge theory [23] we know that the discontinuity across the three-reggeon cut of an odd-signature partial wave is of

the form (we use $\omega = j-1$):

$$disc_\omega F(j,t) = \pi\int d\Omega N_3\delta(\omega-\alpha(k_1)-\alpha(k_2)-\alpha(k_3)+3)N_3\frac{sin(\pi\sum(\alpha(k_i))}{\prod\zeta_{\alpha(k_i)}}, \tag{3.1}$$

where $d\Omega$ denotes the phase space integral over two dimensional momenta, N_3 stands for the three-reggeon vertex, and $\zeta_\alpha = -sin\frac{\pi}{2}(\alpha-1)$ for an odd-signature reggeon. With α from (2.7) the last part of (3.1) becomes, to leading order in g^2:

$$\frac{-\frac{\pi}{2}\sum_i(\alpha(k_i)-1)}{\prod(-\frac{\pi}{2}(\alpha(k_i)-1))}. \tag{3.2}$$

In order to make contact with our approximation of signature factors, we identify:

$$\left(\frac{2}{\pi}N_3\prod_i\sqrt{\frac{1}{\pi\beta(k_i)}}\right)^2 = \sum_{I_{23}}\left(C_3^{(1I_{23};-+)}\right)^2. \tag{3.3}$$

Inserting this into the representation for $T_{2\to2}$ in table 1, we find for the leading real part:

$$\begin{aligned} T_{2\to2}^{(1,-)} = -4\pi^2 s\int\frac{d\omega}{2\pi i}s^\omega\int d\Omega\sum_{I_{23}}C_3^{(1I_{23};-+)}\frac{1}{\omega+3-\alpha(k_1)-\alpha(k_2)-\alpha(k_3)} \\ \cdot\prod_i\left(\frac{1}{-k_i^2-M^2}\right)C_3^{(1I_{23};-+)}. \end{aligned} \tag{3.4}$$

This result is still to be multiplied by the tensor P_1. Remembering the origin of the C_3 vertices, this expression is associated with the diagrams shown in Fig.9a: in the three-reggeon intermediate state, only the even-signature part of the (23)-subsystem contributes, leading to Fig.9b. When calculating from the diagrams of Fig.9a the scattering amplitude, one has to include the overall factor $-4\pi^2$: this minus sign will eventually lead to the famous minus sign of the two-Pomeron cut.

Turning to the even signature t-channels I=0 or I=2, we notice the following. To leading order, the signature factor is purely imaginary, while the partial wave is given by the diagrams shown in Fig.2a. Expanding the signature factor one order beyond the leading one, one finds:

$$\xi_j = -i - \frac{\pi}{2}(\alpha(k_1)+\alpha(k_2)-2). \tag{3.5}$$

At the tip of the two-reggeon cut we therefore expect a contribution of the form:

$$T_{2\to 2} = -2\pi s \int \frac{d\omega}{2\pi i} \int d\Omega C_2^{(I;+)} \frac{-\frac{\pi}{2}(\alpha(k_1)+\alpha(k_2)-2)}{\omega-\alpha(k_1)-\alpha(k_2)+2} \prod_i \left(\frac{1}{-k_i^2-M^2}\right) C_2^{(I;+)}. \tag{3.6}$$

This contribution can again be obtained from the diagrams shown in Fig.9a. First we remember that neither the I=0 nor the I=2 channels have a three reggeon cut ((2.19), and (2.32)-(2.35)). Therefore, if we try to take the discontinuity across the three-reggeon cut, we always meet the cut killing factor. For example, if in the I=0 channel the (23)-subsystem is in the state $(I_{23}=1, \tau_{23}=-)$, the diagrams of Fig.9a can be drawn as shown in Fig.9c:

$$-4\pi^2 - \int \frac{d^2k_1 d^2k_2}{(2\pi)^6} C_2^{(0;+)} \frac{\omega+3-\alpha(k_1)-\alpha(k_2)-\alpha(k_3)}{\omega+2-\alpha(k_2)-\alpha(k_3)} \frac{1}{(\omega+3-\alpha(k_1)-\alpha(k_2)-\alpha(q-k_1-k_2))}$$
$$\cdot \frac{\omega+3-\alpha(k_1)-\alpha(k_2)-\alpha(k_3)}{\omega+2-\alpha(k_2)-\alpha(k_3)} \prod_i \left(\frac{1}{-k_i^2-M^2}\right) C_2^{(0;+)}, \tag{3.7}$$

and the three-reggeon cut obviously cancels. Adopting the point of view that all reggeon diagrams have an unambigous meaning only near singularities in the t-channel (either reggeon or particle discontinuities), we interpret this particular configuration of the (23)-subsystem as the analytic continuation (in $t=-q^2$ and $t_{23}=-(k_2+k_3)^2$) of the two-particle discontinuity in the t_{23} channel. At physical t-values, the remaining cut killing factor in (3.7) equals ω, and the momentum integral in the (23) subsystem is

$$disc_{t_{23}} \beta_2(t_{23}). \tag{3.8}$$

We therefore interpret the integrand as the discontinuity in t_{23} across the two particle cut of

$$-4\pi^2 C_2^{(0;+)} \frac{\alpha(t_{23})-1}{\omega+2-\alpha(t_1)-\alpha(t_{23})} \frac{1}{(t_1-M^2)(t_{23}-M^2)} C_2^{(0;+)}. \tag{3.9}$$

Using a t-dispersion relation in the (23)-subsystem and returning to negative values of t and t_{23}, eq.(3.7) reads:

$$-4\pi^2 \int \frac{d^2k}{(2\pi)^3} C_2^{(0;+)} \frac{1}{\omega+2-\alpha(k_1)-\alpha(k_2)} \frac{-\frac{\pi}{2}(\alpha(k_1)+\alpha(k_2)-2)}{(-k_1^2-M^2)(-k_2^2-M^2)} C_2^{(0;+)}. \tag{3.10}$$

Together with the other configurations in the (23)-subsystem, this leads just to the contribution (3.6) which we expected. Finally it should be noted that the argument which have given here is slightly simplified: a more detailed study of the analytic continuation of the (23) subsystem should use a separate angular momentum variable ω_{23}, i.e. the energy non-conserving vertex functions $C_3^{(01;+-)}(k_1k_2k_3;\omega_1,\omega_{23})$. Its derivation follows closely the discussion of $C_3^{(11;--)}$ in (2.36) - (2.37).

A careful analysis of the diagrams of Fig.9a gives two more contributions, the particle two-reggeon cut in the even signature channel and the three particle cut of the trajectory function in the odd signature, I=1 channel. The latter one is obtained in the same way as scetched in (2.14)-(2.16): start from the three-reggeon intermediate state and consider the $(I_{23}=1;\tau_{23}=-)$ configuration of the (23)-subsystem. With (2.26) we find, after continuation to $t>9M^2$,

$$\omega g \frac{1}{\omega+1-\alpha(t)} disc_t \beta_3(t) \frac{1}{\omega+1-\alpha(t)} g, \tag{3.11}$$

where

$$\beta_3(t) = \frac{\pi^2}{2} g^4 \int \frac{d^2k_1 d^2k_2}{(2\pi)^6} \frac{1}{(-k_1^2-M^2)(-k_2^2-M^2)(-(q-k_1-k_2)^2-M^2)} \tag{3.12}$$

is the three particle contribution to the trajectory function. (3.11) is the same as the three particle discontinuity of

$$g \frac{\alpha-1}{(\omega+1-\alpha(t))(t-M^2)} g, \tag{3.13}$$

if we put

$$\alpha(t) = 1 + (t-M^2)\beta_2(t) + (t-M^2)\beta_3(t). \tag{3.14}$$

Finally, the two-reggeon particle cut in the even signature channels, They come from the configuration $(I_{23}=1;\tau_{23}=+)$, which is a "wrong signature" state. With the results (2.19 and (2.35) we have two "diagonal" contributions which lead to the same result as described above (3.10), but also two "nondiagonal" ones which we interpret as particle-two reggeon discontinuities.

The result of this discussion is stated as follows. Compared to the leading -lns approximation, we are now down by two powers of g^2. In the odd signature channel, a new contribution to the real part has been obtained. It follows from the two particle $\rightarrow$ three reggeon vertex which ahs been discussed in the previous section, and it contains the three reggeon cut. In the even signature channels, we have found the real part, which on the two reggeon branch point singularity matches the leading imaginary part. The peculiar result of this section is the fact that all these contributions (and two others) can be derived from the reggeon diagrams in Fig.9a, provided we consider these diagrams to be defined only in the vicinity of cuts in either momentum or angular momentum. This is an illustration of how self-constrained these diagrams are: in some t-channel configurations (I=0 or 2 and $\tau = +$) the diagrams from Fig.9a with three reggeon lines are closely related to those from Fig 2 with only two lines. In another state (I=1 and $\tau = -$) the same diagrams give "something new", namely the three reggeon cut. This already indicates how we shall continue: by increasing, step by step, the number of reggeon lines in the t-channel, we find new contributions (higher reggeon cuts) but also real or imaginary parts which match previous steps.

This would also be the place to adress the question of the infrared behavior in the vacuum exchange channel. However, in order to make this paper not too long, we only mention the result: provided the coupling of the reggeon lines to external particles is replaced by a suitable quark loop, it can be shown that the diagrams are finite in the limit of zero boson mass. The proof makes use of the representations for $K_{2\rightarrow 2}$, and $K_{2\rightarrow 3}$ which are given in the appendix of II and follows the analogous proof for the Lipatov ladders. It will be presented in a separate paper.

We generalize our result on the three-reggeon cut in $T_{2\rightarrow 2}$ to inelastic production amplitudes, but do not (yet) attempt to carry out an analysis analogous to the elastic case. Support for our argument will come in the next section. For the amplitude $T_{2\rightarrow 3}$ we expect new contributions to the real parts for all signature combinations. For the case $\tau_1 = \tau_2 = -$

the three reggeon cut (as well the three particle state in the trajectory function) must appear, for all other combinations the real part can be derived from the known (imaginary) amplitudes of previous steps. In analogy with the elastic case we conjecture that all these contributions can be derived from the diagrams of Fig.9a by attaching a production vertex at all possible places. A similar result is conjectured for multiparticle amplitudes $T_{2\rightarrow 4}$ etc.

4 Triple Discontinuities and Four-Reggeon Vertices

The next step in the construction scheme are the production amplitudes $T_{2\rightarrow 4}$ and $T_{3\rightarrow 3}$ (Table 1). The determination of their partial waves requires triple energy discontinuities, which lead to four reggeon vertex functions. In close analogy with section III we define amputated vertex functions C_4 and nonamputated functions (Green's functions) D_4. When introducing signature and group structure, we first need to define the order in which particles (or reggeons) are coupled together. There are two different schemes (Fig.10a and b), and we will denote them by the superscripts $(II_{12}I_{34};\tau,\tau_{12}\tau_{34})$ and $(II_{234}I_{34};\tau\tau_{234}\tau_{34})$, resp. Calculations of tensors are again defered into the appendix. Integral equations for the Green's function D are illustrated in Fig.11; before they can be written down explicitly, we have to reduce the group structure. We first define normalized tensors $P_{II_{12}I_{34}}$ etc, then amplitudes with definite isospin and signature $C_4^{(II_{12}I_{34};\tau,\tau_{12}\tau_{34})} \cdot P_{II_{12}I_{34}}$ etc (signature is, again, the parity under exchanging simultaneously group indices and momenta of reggeon or particle lines), and finally decompose the equation illustrated in Fig.11 into sets of coupled integral equations. Because of their large number, they will not be written out in detail, but all necessary ingredients are given in the appendix. We limit our discussion to a few cases, which are of special interest, and present their solutions.

Following our analysis of the three-reggeon vertex function, we first should discuss the partial waves of $T_{2\rightarrow 4}$ and $T_{3\rightarrow 3}$ and check their consistency with the single energy discontinuities from II. Because of the large number of different signature combinations, we do not attempt to present a complete discussion. We only mention that, for the

case of negative signature in all three t-channels, we find complete agreement with the results from I and II. The most interesting case are the partial waves F_{31} and F_{13}. They present, conceptually, a new step, namely n-reggeon $\rightarrow$ m-reggeon vertex functions (with one incoming and one outgoing reggeon being taken on the particle pole). A detailed discussion is deferred to the subsequent paper where we will start to "iterate" in the t-channel. For the time being we only mention that when inserting the results for the partial waves into the representations of Table 1 and then expanding the signature factors in powers of g^2, we obtain the leading real part of (2.1). In addition, we get next-to-leading and next-next-to leading contributions which can be represented as diagrams with two or three regeon lines, resp..

Next we turn to $T_{2\to 2}$ in the $(I=1,\tau=-)$ channel. The question we are interested in is s-channel unitarity of $T_{2\to 2}$. To be more precise, we wish to demonstrate that the new real part which we constructed in the previous section matches the imaginary part which can be obtained from unitarity equations. To this end let us return to eq.(2.4) and the discussion thereafter. Compared to the leading-lns approximation (2.1), the real part of the previous section is down by two powers of g^2. If we denote this by subscript "nnl" (=next-next-to-leading), the generalization of (2.4) that we have to verify is:

$$disc_s T_{2\to 2}^{(nnl)} = \frac{1}{2}\sum_{n=2}^{\infty}\int d\Omega_n \left(T_{2\to n}^{(nnl)}T_{2\to n}^{*(l)} + T_{2\to n}^{(nl)}T_{2\to n}^{*(nl)} + T_{2\to n}^{(l)}T_{2\to n}^{*(nnl)}\right). \qquad (4.1)$$

For $T^{(l)}$ we use (2.1), for $T^{(nl)}$ use the amplitude in table 1, substitute the results for the partial waves from section III and expand the signature factors. For $T^{(nnl)}$ we have the new contributions from the previous section, but also subleading terms from the partial waves in section III. Diagrammatically, the sum on the rhs of eq.(4.1) can be summarized as shown in Fig.12: all three terms are identical, but since the first and the third terms have a relative minus sign, the sum comes with an overall factor (-1). Restricting ourselves in (4.1) to the channel $(I=1,\tau=-)$, we verify that it contains (among other contributions) the imaginary part that matches the real part of section III.

To see this in more detail we look at the discontinuity across the four-reggeon cut

(Fig.12) and project on the following t-channel configurations (remember that in the discussion of the three reggeon cut in the previous section, we have chosen the coupling scheme of Fig.4, i.e.the two lower reggeons "2" and "3" are coupled to an even-signature state):

1) the pair (34) is in an $(i=1,\tau=-)$ state, the system ((34)2) in a $(\tau=+)$ state; this requires, in the coupling scheme of Fig.10a, the amplitude $C_4^{(1I_{234}1;--+)}$;

2) the pair (23) is in an $(i=1,\tau=-)$ state, the system (4(23)) in a $(\tau=+)$ state; for this we need, again in the coupling scheme of Fig.10b, the amplitude $C_4^{(1I_{234}1;-+-)}$;

3) the pair (12) is in an $(i=1,\tau=-)$ state, the system (34) in a $(\tau=+)$ state; this case belongs to the scheme of Fig.10a, and requires $C_4^{(11I_{34};--+)}$.

Here we do not want to give the integral equations in all detail; all necessary ingredients for writing down the equations are given in the appendix. We only quote those solutions which are of interest for us:

$$\begin{aligned} C_4^{(1I_{234}1;-+-)}(k_1k_2k_3k_4;\omega) &= C_3^{(1I_{234};-+)}(k_1,k_2,k_3+k_4;\omega) \\ &\cdot\frac{\omega+4-\alpha(k_1)-\alpha(k_2)-\alpha(k_3)-\alpha(k_4)}{\omega+3-\alpha(k_1)-\alpha(k_2)-\alpha(k_3+k_4)}\cdot g \qquad (4.2)\\ C_4^{(1I_{234}1;-+-)}(k_1k_2k_3k_4;\omega) &= C_3^{(1I_{234};-+)}(k_1,k_2+k_3,k_4;\omega) \\ &\cdot\frac{\omega+4-\alpha(k_1)-\alpha(k_2)-\alpha(k_3)-\alpha(k_4)}{\omega+3-\alpha(k_1)-\alpha(k_2+k_3)-\alpha(k_4)}\cdot g \qquad (4.3)\\ C_4^{(11I_{34};--+)}(k_1k_2k_3k_4;\omega) &= C_3^{(1I_{34};-+)}(k_1+k_2,k_3,k_4;\omega) \\ &\cdot\frac{\omega+4-\alpha(k_1)-\alpha(k_2)-\alpha(k_3)-\alpha(k_4)}{\omega+3-\alpha(k_1+k_2)-\alpha(k_3)-\alpha(k_4)}\cdot g. \qquad (4.4)\end{aligned}$$

With these results we repeat the argument made in (3.6) and (3.7); the would-be four-reggeon discontinuity turns into the expression (cf.(3.10)):

$$-\frac{1}{2}\omega\int\frac{d^2k_1d^2k_2}{(2\pi)^6}C_3^{(1I_{23};-+)}\frac{\pi(\alpha(k_1)+\alpha(k_2)+\alpha(k_3)-3)}{\omega+3-\alpha(k_1)-\alpha(k_2)-\alpha(k_3)}\prod_i\left(\frac{1}{-k_i^2-M^2}\right)C_3^{(1I_{23};-+)}. \qquad (4.5)$$

For each single I_{23}, this is exactly the partial wave which matches (3.4): we therefore have shown that our real part from section III "bootstraps" itself. This again illustrates the consistency between D_3 and D_4 and represents one of the key features of our whole construction scheme.

The other case of interest is the vacuum channel ($I = 0, \tau = +$). Here we slightly generalize and consider, apart from $T_{2\to 2}$, also $T_{3\to 3}$ in the triple Regge limit (Fig.13a). From the representation given in table 1 we see that we need a triple energy discontinuity, which leads directly to the energy nonconserving four-reggeon vertices with the three energy variables ω, ω_1, ω_2 for the channels t, t_1, and t_2, resp. Quantum number assignments are $(0,+)$ in the t-channel, and $I_1 = I_2 = 0,1,2$ and $\tau_1 = \tau_2 = +,-$ for the t_1 and t_2 channels. Following the discussion of section II.2 we first discuss the energy conserving case, then generalize to $\omega_1 + \omega_2 \neq \omega$. Using all the ingredients given in the appendix, we have the following two sets of integral equations:

$$
\begin{aligned}
\omega D_4^{(000;+++)} &= -\tfrac{4}{\sqrt{3}} g^4 + \tfrac{4}{\sqrt{3}} D_2^{(0;+)} \otimes K_{2\to 4}(\{k_1k_2\}\{k_3k_4\}) \\
&-2\sqrt{\tfrac{2}{3}} \Big(D_3^{(01;++)}(k_a[k_bk_4]) \otimes K_{2\to 3}(\{k_1k_2\}k_3) + D_3^{(01;++)}(k_a[k_bk_3]) \otimes K_{2\to 3}(\{k_1k_2\}k_4) \\
&+D_3^{(01;++)}([k_1k_a]k_b) \otimes K_{2\to 3}(k_2\{k_3k_4\}) + D_3^{(01;++)}([k_2k_a]k_b) \otimes K_{2\to 3}(k_1\{k_3k_4\}) \Big) \\
&+D_4^{(000;+++)} \otimes (-2K_{2\to 2}(k_1k_2) - 2K_{2\to 2}(k_3k_4) + \textstyle\sum \alpha(k_i) - 4) \\
&+D_4^{(011;+++)} \otimes \tfrac{2}{\sqrt{3}} (K_{2\to 2}(k_2k_3) - K_{2\to 2}(k_1k_3) - K_{2\to 2}(k_2k_4) + K_{2\to 2}(k_1k_4)),
\end{aligned}
\tag{4.6}
$$

$$
\begin{aligned}
\omega D_4^{(011;+++)} &= -D_2^{(0;+)} \otimes K_{2\to 4}([k_1k_2][k_3k_4]) \\
&+\tfrac{1}{\sqrt{2}} \Big(D_3^{(01;++)}(k_a[k_bk_4]) \otimes K_{2\to 3}([k_1k_2]k_3) - D_3^{(01;++)}(k_a[k_bk_3]) \otimes K_{2\to 3}([k_1k_2]k_4) \\
&+D_3^{(01;++)}([k_1k_a]k_b) \otimes K_{2\to 3}(k_2[k_3k_4]) - D_3^{(01;++)}([k_2k_a]k_b) \otimes K_{2\to 3}(k_1[k_3k_4]) \Big) \\
&+D_4^{(000;+++)} \otimes \tfrac{2}{\sqrt{3}} (K_{2\to 2}(k_2k_3) - K_{2\to 2}(k_1k_3) - K_{2\to 2}(k_2k_4) + K_{2\to 2}(k_1k_4)) \\
&+D_4^{(011;+++)} \otimes (-K_{2\to 2}(k_1k_2) - K_{2\to 2}(k_3k_4) + \textstyle\sum \alpha(k_i) - 4 \\
&-\tfrac{1}{2}K_{2\to 2}(k_2k_3) - \tfrac{1}{2}K_{2\to 2}(k_1k_3) - \tfrac{1}{2}K_{2\to 2}(k_2k_4) - \tfrac{1}{2}K_{2\to 2}(k_1k_4)) \\
&+D_4^{(022;+++)} \otimes \tfrac{1}{2}\sqrt{\tfrac{5}{3}} (K_{2\to 2}(k_2k_3) - K_{2\to 2}(k_1k_3) - K_{2\to 2}(k_2k_4) + K_{2\to 2}(k_1k_4)),
\end{aligned}
\tag{4.7}
$$

$$
\begin{aligned}
\omega D_4^{(022;+++)} &= -\sqrt{\tfrac{5}{3}} g^4 + \sqrt{\tfrac{5}{3}} D_2^{(0;+)} \otimes K_{2\to 4}(\{k_1k_2\}\{k_3k_4\}) \\
&-\sqrt{\tfrac{5}{6}} \Big(D_3^{(01;++)}(k_a[k_bk_4]) \otimes K_{2\to 3}(\{k_1k_2\}k_3) + D_3^{(01;++)}(k_a[k_bk_3]) \otimes K_{2\to 3}(\{k_1k_2\}k_4) \\
&+D_3^{(01;++)}([k_1k_a]k_b) \otimes K_{2\to 3}(k_2\{k_3k_4\}) + D_3^{(01;++)}([k_2k_a]b) \otimes K_{2\to 3}(k_1\{k_3k_4\}) \Big) \\
&+D_4^{(011;+++)} \otimes \tfrac{1}{2}\sqrt{\tfrac{5}{3}} (K_{2\to 2}(k_2k_3) - K_{2\to 2}(k_1k_3) - K_{2\to 2}(k_2k_4) + K_{2\to 2}(k_1k_4)) \\
&+D_4^{(022;+++)} \otimes (+K_{2\to 2}(k_1k_2) + K_{2\to 2}(k_3k_4) + \textstyle\sum \alpha(k_i) - 4 \\
&-\tfrac{2}{3}[K_{2\to 2}(k_2k_3) - K_{2\to 2}(k_1k_3) - K_{2\to 2}(k_2k_4) + K_{2\to 2}(k_1k_4)] \Big),
\end{aligned}
\tag{4.8}
$$

and

$$
\begin{aligned}
\omega D_4^{(000;+--)} &= +\tfrac{4}{\sqrt{3}} D_2^{(0;+)} \otimes K_{2\to 4}([k_1k_2][k_3k_4]) \\
&-2\sqrt{\tfrac{2}{3}} \Big(D_3^{(01;+-)}(k_a\{k_bk_4\}) \otimes K_{2\to 3}([k_1k_2]k_3) - D_3^{(01;+-)}(k_a\{k_bk_3\}) \otimes K_{2\to 3}([k_1k_2]k_4) \\
&+D_3^{(01;+-)}(\{k_1k_a\}k_b) \otimes K_{2\to 3}(k_2[k_3k_4]) - D_3^{(01;+-)}(\{k_2k_a\}k_b) \otimes K_{2\to 3}(k_1[k_3k_4]) \Big) \\
&+D_4^{(000;+--)} \otimes (-2K_{2\to 2}(k_1k_2) - 2K_{2\to 2}(k_3k_4) + \textstyle\sum \alpha(k_i) - 4) \\
&+D_4^{(011;+--)} \otimes \tfrac{2}{\sqrt{3}} (K_{2\to 2}(k_2k_3) - K_{2\to 2}(k_1k_3) - K_{2\to 2}(k_2k_4) + K_{2\to 2}(k_1k_4)),
\end{aligned}
\tag{4.9}
$$

$$
\begin{aligned}
\omega D_4^{(011;+--)} &= g^4 - D_2^{(0;+)} \otimes K_{2\to 4}(\{k_1k_2\}\{k_3k_4\}) \\
&+\tfrac{1}{\sqrt{2}}\Big(D_3^{(01;+-)}(k_a\{k_bk_4\}) \otimes K_{2\to 3}(\{k_1k_2\}k_3) + D_3^{(01;+-)}(k_a\{k_bk_3\}) \otimes K_{2\to 3}(\{k_1k_2\}k_4) \\
&+D_3^{(01;+-)}(\{k_1k_a\}k_b) \otimes K_{2\to 3}(k_2\{k_3k_4\}) + D_3^{(01;+-)}(\{k_2k_a\}k_b) \otimes K_{2\to 3}(k_2\{k_3k_4\})\Big) \\
&+D_4^{(000;+--)} \otimes \tfrac{2}{\sqrt{3}}\left(K_{2\to 2}(k_2k_3) - K_{2\to 2}(k_1k_3) - K_{2\to 2}(k_2k_4) + K_{2\to 2}(k_1k_4)\right) \\
&+D_4^{(011;+--)} \otimes \Big(-K_{2\to 2}(k_1k_2) - K_{2\to 2}(k_3k_4) + \textstyle\sum \alpha(k_i) - 4 \\
&-\tfrac{1}{2}K_{2\to 2}(k_2k_3) - \tfrac{1}{2}K_{2\to 2}(k_1k_3) - \tfrac{1}{2}K_{2\to 2}(k_2k_4) - \tfrac{1}{2}K_{2\to 2}(k_1k_4)\Big) \\
&+D_4^{(022;+--)} \otimes \tfrac{1}{2}\sqrt{\tfrac{5}{3}}\left(K_{2\to 2}(k_2k_3) - K_{2\to 2}(k_1k_3) - K_{2\to 2}(k_2k_4) + K_{2\to 2}(k_1k_4)\right),
\end{aligned}
\tag{4.10}
$$

$$
\begin{aligned}
\omega D_4^{(022;+--)} &= \sqrt{\tfrac{5}{3}}D_2^{(0;+)} \otimes K_{2\to 4}([k_1k_2][k_3k_4]) \\
&-\sqrt{\tfrac{5}{6}}\Big(D_3^{(01;+-)}(k_a\{k_bk_4\}) \otimes K_{2\to 3}([k_1k_2]k_3) - D_3^{(01;+-)}(k_a\{k_bk_3\}) \otimes K_{2\to 3}([k_1k_2]k_4) \\
&+D_3^{(01;+-)}(\{k_1k_a\}k_b) \otimes K_{2\to 3}(k_2[k_3k_4]) - D_3^{(01;+-)}(\{k_2k_a\}k_b) \otimes K_{2\to 3}(k_1[k_3k_4])\Big) \\
&+D_4^{(011;+--)} \otimes \tfrac{1}{2}\sqrt{\tfrac{5}{3}}\left(K_{2\to 2}(k_2k_3) - K_{2\to 2}(k_1k_3) - K_{2\to 2}(k_2k_4) + K_{2\to 2}(k_1k_4)\right) \\
&+D_4^{(022;+--)} \otimes \Big(+K_{2\to 2}(k_1k_2) + K_{2\to 2}(k_3k_4) + \textstyle\sum \alpha(k_i) - 4 \\
&+\tfrac{2}{3}[K_{2\to 2}(k_2k_3) - K_{2\to 2}(k_1k_3) - K_{2\to 2}(k_2k_4) + K_{2\to 2}(k_1k_4)]\Big).
\end{aligned}
\tag{4.11}
$$

There is one new element in these equations, the interaction kernel $K_{2\to 4}$. It has the form (cf.eq.(2.14) and II,eq.(A.17)):

$$
\begin{aligned}
\frac{1}{g^4}K_{2\to 4}(k_1k_2;k_1'k_2'k_3'k_4') &= -(-q^2 - \frac{15}{8}M^2) \\
&+\frac{(-(k_1'+k_2'+k_3')^2 - \frac{7}{4}M^2)(-k_2^2 - M^2)}{-(k_2-k_4')^2 - M^2} + \frac{(-(k_2'+k_3'+k_4')^2 - \frac{7}{4}M^2)(-k_1^2 - M^2)}{-(k_1-k_1')^2 - M^2} \\
&-\frac{(-k_1^2 - M^2)(-k_2^2 - M^2)(-(k_2'+k_3')^2 - \frac{3}{2}M^2)}{(-(k_1-k_1')^2 - M^2)(-(k_2-k_4')^2 - M^2)}.
\end{aligned}
\tag{4.12}
$$

As to the solutions of these equations, we only remark the following: in the first set of equations (even signature) there is no reason to expect that any pair of the outgoing reggeons should "collaps". It is only in the three reggeon intermediate state where we need a modification: indeed, eq.(2.19) tells us that there is no three reggeon cut, i.e.the diagrams could be redrawn as in Fig.13b. For the second set of equations we simply find:

$$
\begin{aligned}
D_4^{(011;+--)}(k_1k_2k_3k_4;\omega) &= \frac{1}{2}D_2^{(0;+)}(k_1+k_2,k_3+k_4;\omega)\cdot g^2 \\
D_4^{(000;+--)}(k_1k_2k_3k_4;\omega) &= 0 \\
D_4^{(022;+--)}(k_1k_2k_3k_4;\omega) &= 0.
\end{aligned}
\tag{4.13}
$$

The transition to the energy nonconserving vertices is done as demonstrated in section III: first one defines the "last" vertex, the branching vertex. To the right of it, we have the D_4 functions from above, to the left the Green's function of the two reggeon channel. From these building blocks we obtain the desired results.

The energy nonconserving vertex function $C_4^{(000;+++)}(k_1,..,k_4;\omega,\omega_1,\omega_2)$ allows to define the triple Pomeron vertex (to leading order): all three t-channels contain the fixed-cut singularity found first by Lipatov et al., and its residue could be used to define a triple Pomeron vertex. It is, however, clear from our analysis that the t-channel contains also the four-reggeon cut which has a new fixed-cut singularity somewhere to the right of j=1: the splitting of one "bare" Pomeron into two "bare" Pomerons cannot be seperated from a new contribution to the "bare" Pomeron.

Returning now to $T_{2\to 2}$ in the vacuum channel (Fig.12), we could isolate the "double Pomeron" exchange by taking the discontinuity across the four reggeon cut and forming the states $I_{12} = I_{34} = 0$, and $\tau_{12} = \tau_{34} = +$ in the t_{12} and t_{34} channels. The negative sign of this contribution can be traced back to eq.(4.1): the middle term which is positive contains both the diffractive and double multiperipheral energy cut (the identification of the latter one requires a recoupling of the four reggeon state into two Pomerons), whereas the first and the third terms lead to the negative multiperipheral cut.

There is an interesting application of this contribution to the vacuum exchange channel, namely deep inelastic scattering. In the same way as it is possible to derive from the two-reggeon ladder the leading small-x behavior of the deep inelastic structure function, one might try to derive from the diagrams in Fig.14 the first so-called fan diagram of Gribov, Levin, and Ryskin [9]. The idea would be to replace at the left end of Fig.12, the particle vertex by a closed quark loop with deep inelastic external photons (mass $-q^2 = Q^2$); then remove the gluon mass (which gives a finite answer), and finally take the limit of large Q^2. One expects to see two major simplifications: the right part of the diagrams with three or two reggeons shrink to a "pointlike" vertex, whereas in the four reggeon state the reggeons are grouped into two color singlet pairs. This problem will be treated in a forthcoming paper.

5 Generalizations

After these somewhat detailed discussions of the particle $\to$ reggeon vertexfunctions D_3 and D_4 we try to generalize to the two-particle $\to$ n-reggeon vertexfunction D_n. The structure of the integral equation can be obtained most easily from Fig.3c or Fig.11. Starting from the left end of the diagrams, the number of reggeon lines never deceases. The interaction kernels are $K_{2\to 2}$, $K_{2\to 3}$, $K_{2\to 4}$,...,$K_{2\to n}$, and we have to sum over all possibilities. The analytic form of the kernels is obtained from the prescription given in the appendix of II and will not be repeated here. We only quote the particularly simple form of the zero-mass limit (Fig.17):

$$K_{2\to n} = 2g^n(-1)^n(k_1' + r_1\frac{k_1'^2}{r_1^2})_i T_{ij}(r_1)T_{jl}(r_2)(k_2' + r_2\frac{k_2'^2}{r_2^2})_l, \tag{5.1}$$

where

$$T_{ij}(r) = \delta_{ij} - 2\frac{r_i r_j}{r^2}. \tag{5.2}$$

Based upon the experience with D_3 and D_4 we expect these leading order functions D_n to possess "bootstrap" properties, similar to those found in this paper. We have not

yet tried to find a systematic list of such identities. It is, however, quite simple to verify the simplest one: whenever two adjacent reggeon lines are in a $(I = 1, \tau = -)$ state, they "collapse" to a single reggeon line. This identity can be proven without forming fully signatured and group-reduced amplitudes. Repeating this procedure several times, one finds strings of relations between D_n, D_{n-1},... and D_2. There is no doubt that more general relations exist (e.g.(2.34)), which garantuee that for even (odd) signature in the total t-channel only reggeon-cut singularities with even (odd) numbers of reggeon lines exist: this implies that the D_n's can be cast into a form which satisfies the rules of reggeon unitarity.

For later applications it might be useful to stress again that these two-particle $\to$ n-reggeon vertexfunctions can be written in several equivalent ways: either one uses the form which arises directly from multiple energy discontinuities (at this stage we have reggeon propagators in the t-channels, and no reduction of the group structure or decomposition into signatured states has taken place). Now we have two alternatives: either we rewrite the integral equations in such a way that instead of the reggeon propagators we get elementary particle propagators: this form is most useful for studying the zero mass limit. One also is closest to the attractive idea of formulating the high energy limit of QCD as an effective two-dimensional conformal field theory [24]. Alternatively one may decide to introduce signature: then the "bootstrap" equations ensure that one obtains a reggeon field theory (with momentum dependent, i.e.nonlocal vertices). In particluar, one of the basic rules of Regge theory, the signature conservation law, is restored. In this paper, we have made use of all these different ways of writing the vertex functions.

Knowing the two-particle $\to$ n-reggeon vertices, one constructs partial waves and scattering amplitudes. For the most interesting case, $T_{2\to 2}$, we expect the following hierarchy. If we draw the reggeon diagrams as they come from multiple energy discontinuities, i.e. we do not yet decompose the group tensors or form signatured amplitudes, then diagrams with up to 2n-1 reggeon lines (n=1,2,...), give real parts, those with up to 2n lines imag-

inary amplitudes. At the leading j-plane singularity, i.e. the cut corresponding to the maximal number of reggeons in the t-channel, we look at definite isospin and signature in the t-channel and in sub-t-channels: analogoulsly to the few cases which we have studied in detail, this procedure may "reduce" the number of reggeon lines, thus providing a non-leading contribution to another reggeon diagram with fewer lines. In other cases we expect higher order contributions to the trajectory function etc.

Eventually we will have to sum up all these diagrams, in particular we wish to find the leading j-plane singularity in the vacuum exchange channel (Pomeron). In order to avoid double counting, it seems useful to start from that form of the amplitude where no "contraction of lines" has yet been performed. As we have demonstrated, this form when decomposed into irreducible group tensors and signatured amplitudes, is really a sum of several different reggeon diagrams. Among others, one also obtains corrections to the trajectory function and internal signature factors.

A more subtle point arises in connection with the real part. From the point of view of Regge theory, the dynamical information is contained in the partial wave, and real and imaginary parts of the amplitude follow from the signature factors. Our way of construction, however, at first sight seems to build real and imaginary parts independently from each other. It is then the role of the "bootstrap" equations which ensures that they match, at least near the leading multiregge cut singularities. Consequently, we may feel allowed to simply disregard the real parts altogether: the imaginary parts (more precisely: energy discontinuities) are sufficient to determine the partial waves, and the rest follows from the signature factors. This remains correct as long as we confine ourselves to the multiregge cut singularities where the consistency has been verified. However, as soon as we ask for bound states of two or more reggeons, this consistency, strictly speaking, is lost. For example, the leading vacuum singularity of the diagrams of Fig.2 (belonging to the imaginary part of $T_{2\to 2}$ is different from that of Fig.9a in the vacuun channel. The only hope to resolve this difficulty lies in the fact that neither of them is physical: a reliable

answer for the Pomeron singularity can be obtained only from summing over all diagrams, i.e. after finding the bound state of infinitely many reggeons.

Finally we say a few words about the last part of this program. The present paper has defined and investigated two-particle $\to$ n-reggeon vertices (to leading order in g^2), and their contribution to partial waves. The obvious missing step is the "iteration in the t-channel", i.e. the inclusion of those reggeon diagrams where the number of reggeons in the t-channel increases and decreases repeatedly. Formally speaking, the partial amplitudes and partial waves discussed in this paper satisfy reggeon unitarity only in a very restricted sense. What is needed are n-reggeon $\to$ m-reggeon amplitudes. The first place where one encounters such an amplitude is the $2 \to 4$ scattering amplitude, more precisely the partial waves F_{13} and F_{31} (Table 1). Their discussion will be subject of the final part of this program. Connected with this step is another contribution which we have encountered already in this paper: the "cut" production vertex (2.53). When inserting this real-valued contribution to the production amplitude into the unitarity equations, one finds a new contribution to the kernel $K_{2\to 2}$ (vertex correction). In the present context this contribution does not seem to participate in the bootstrap equations: in terms of powers of g^2, however, there is no justification to disregard this term. From the point of view of unitarity, it should come in together with the higher order particle thresholds in the trajectory function.

6 Summary and Discussion

This paper contains part of a systematic attempt to go beyond the leading lns approximation of the Regge limit in a nonabelian gauge theory. The underlying idea is to give more weight to the (formal) property of unitarity in both the s and t-channel rather than trying to obtain a complete set of, say, all next-to-leading lns terms.

The central topic of this paper was the discussion of two-particle $\to$ n-reggeon amplitudes. The are obtained from multiple energy discontinuities, and after the decomposition

of the group structure and the introduction of signature one finds "bootstrap" properties which ensure that these amplitudes can always be written as reggeon field theory diagrams. In this sense, the "bootstrap" properties are consequences of the reggeization of the vector particle. As to the reggeon field theory, these particle-reggeon amplitudes allow to find new elements: in this paper, we have discussed explicitly the (momentum dependent) reggeon $\rightarrow$ three-reggeon vertex, the triple Pomeron vertex, the three-particle contribution to the trajectory function. and a "vertex correction" to the $2 \rightarrow 2$ reggeon kernel. With the help of these amplitudes we then have constructed partial waves with three and four-reggeon cut singularities, and we have demonstrated that s-channel unitarity equations are satisfied if we move onto the (leading) reggeon cut singularities.

As it has been outlined in the final section, there is still on major step to be taken, namely the construction of m-reggeon $\rightarrow$ n-reggeon amplitudes. This will be the content of a forthcoming paper. The present paper also does not contain the proof that the amplitudes D_n are infrared finite in the vacuum channel: this will be shown in a separate paper. These investigations will be based upon the non-signatured two-particle $\rightarrow$ n-reggeon amplitudes which are derived and discussed in this paper.

Once this program of extracting from perturbation theory a set of unitary high energy amplitudes has been completed, we shall be confronted with the task of calculating the leading bound state singularity in the vacuum channel, the Pomeron. We think that the solution to this problem will go beyond perturbation theory. On the other hand it is hoped that since this set of perturbative contributions is already so much constrained by its unitarity properties, it contains already substantial information on the structure of the full theory. In principle the form of the amplitudes as they are derived in this paper offers different ways of attacking the bound state problem: either reggeon field theory [25] or two-dimensional conformal field theory [24]. For the latter method the results of this (and the subsequent) paper have to be used to formulate such a field theory.

Acknowledgements

In an early stage of this work I had helpful discussions with A.R.White which are greatfully acknowledged. This paper was completed while I have been visiting the Lund University: I would like to thank Bo Anderson and his group for their warm hospitality extended to me.

Note added: After this paper had been completed I received a paper of L.Lipatov (Orsay-preprint IPNO/TH 91-21) which also aims at a unitary high energy desciption of QCD. A detailed comparison of his proposal and the result of this paper seems not very easy but will certainly be of high interest.

APPENDIX: SU(2) TENSOR ALGEBRA

In this appendix we collect a few formula which are useful for the decomposition described in the main part. We begin with a repeat of the case $2 \to 2$ (for the discussion in this appendix there is no need to distinguish between reggeons and particles). Projection operators $P_I(a_1, b_1; a_2, b_2)$ for isospin 0, 1, 2 are defined (I,eq.(4.3)) by:

$$\begin{aligned} P_0(a_1, b_1; a_2, b_2) &= \frac{1}{3}\delta_{a_1 b_1}\delta_{a_2 b_2} \\ P_1(a_1, b_1; a_2, b_2) &= \frac{1}{2}\epsilon_{a_1 b_1 c}\epsilon_{a_2 b_2 c} \\ P_2(a_1, b_1; a_2, b_2) &= \frac{1}{2}\left(\delta_{a_1 a_2}\delta_{b_1 b_2} + \delta_{a_1 b_2}\delta_{a_2 b_1} - \frac{2}{3}\delta_{a_1 b_1}\delta_{a_2 b_2}\right) \end{aligned} \tag{A.1}$$

with

$$P_I(a_1 b_1; a_2 b_2) P_{I'}(a_2 b_2; a_3 b_3) = \delta_{II'} P_I(a_1 b_1; a_3 b_3). \tag{A.2}$$

We shall also use the shorthand notation:

$$P_I P_{I'} = \delta_{II'} P_I. \tag{A.3}$$

Another property is the completeness:

$$\sum_{I=0}^{3} P_I = 1. \tag{A.4}$$

With these projection operators we decompose the group factors $t_{2\to 2}(a_1 b_1; a_2 b_2)$ of the kernel $K_{2\to 2}$ in the integral equation (cf.(I,4.6)) into irreducible representations. With

$$t_{2\to 2}(a_1 b_1; a_2 b_2) = \epsilon_{a_1 c a_2}\epsilon_{c b_1 b_2} \tag{A.5}$$

one obtains:

$$t_{2\to 2} = -2P_0 - P_1 + P_2. \tag{A.6}$$

Next we come to the case $2 \to 3$. Within the coupling scheme of Fig.4a, we define normalized transition tensors $T_{I,I_{23}}$. The normalization is such that

$$T_{I,I_{23}} \cdot T_{I',I'_{23}} = \delta_{I,I'}\delta_{I_{23},I'_{23}} \cdot P_I. \tag{A.7}$$

For (I, I_{23}) we have six possibilites: (0,1), (1,0), (1,1), (1,2), (2,1), (2,2). The tensors have the form:

$$\begin{aligned} T_{01}(a_1 b_1 a_2 b_2 c_2) &= \frac{1}{\sqrt{18}}\delta_{a_1 b_1}\epsilon_{a_2 b_2 c_2} \\ T_{10}(a_1 b_1 a_2 b_2 c_2) &= \frac{1}{\sqrt{6}}\epsilon_{a_1 b_1 a_2}\delta_{b_2 c_2} \\ T_{11}(a_1 b_1 a_2 b_2 c_2) &= \frac{1}{\sqrt{8}}\epsilon_{a_1 b_1 r}\epsilon_{r s a_2}\epsilon_{s b_2 c_2} \\ T_{12}(a_1 b_1 a_2 b_2 c_2) &= \sqrt{\frac{3}{10}}\epsilon_{a_1 b_1 r} P_2(a_2 r; b_2 c_2) \\ T_{21}(a_1 b_1 a_2 b_2 c_2) &= \frac{1}{\sqrt{2}} P_2(a_1 b_1; a_2 l)\epsilon_{l b_2 c_2} \\ T_{22}(a_1 b_1 a_2 b_2 c_2) &= \sqrt{\frac{2}{3}} P_2(a_1 b_1; n m)\epsilon_{a_2 n l} P_2(l m; b_2 c_2). \end{aligned} \tag{A.8}$$

Now we decompose the group part $t_{2\to 3}$ of the kernel $K_{2\to 3}$, which is of the form:

$$t_{2\to 3}(a_1 b_1; a_2 b_2 c_2) = \epsilon_{a_1 l a_2}\epsilon_{l m b_2}\epsilon_{m b_1 c_2}. \tag{A.9}$$

We obtain:

$$t_{2\to 3} = \sqrt{2}T_{01} - \sqrt{\frac{8}{3}}T_{10} + \frac{1}{\sqrt{2}}T_{11} - \sqrt{\frac{5}{6}}T_{12} - \frac{1}{\sqrt{2}}T_{21} - \sqrt{\frac{3}{2}}T_{22}. \tag{A.10}$$

In order to obtain coupled integral equations for reggeon amplitudes with definite isospin, we need to know the weight of the $2 \to 2$ kernels in the different isospin channels of the three-reggeon states (recoupling coefficients). They are listed in table 2. The numbers in the first three columns denote the values (I, I'_{23}, I_{23}), the other three columns contain the coefficents $c^{I}_{I'_{23},I_{23}}$ for the pairwise interaction of the lines (12), (23), (13), resp. (blanks stand for zeroes). These coefficients multiply the kernels $K_{2\to 2}$ in the integral equation Fig.3 (eqs.(2.17)-(2.18), (2.20)-(2.25), (2.28)-(2.31)).

Next we come to the case $2 \to 4$. Here a new feature arises: there exist two different coupling schemes (Fig.10a and b). Let us first consider that of Fig.10a. We again define normalized transition tensors $T_{2\to 4}$ which satisfy

$$T_{I,I_{12},I_{34}} \cdot T_{I',I'_{12},I'_{34}} = \delta_{II'}\delta_{I_{12}I'_{12}}\delta_{I_{34}I'_{34}} P_I. \tag{A.11}$$

We have fifteen possibilities. In components, these tensors are:

$$
\begin{aligned}
T_{000}(a_1b_1;a_2b_2c_2d_2) &= \frac{1}{3\sqrt{3}}\delta_{a_1b_1}\delta_{a_2b_2}\delta_{c_2d_2}\\
T_{011}(a_1b_1;a_2b_2c_2d_2) &= \frac{1}{6}\delta_{a_1b_1}\epsilon_{a_2lb_2}\epsilon_{ld_2c_2}\\
T_{022}(a_1b_1;a_2b_2c_2d_2) &= \frac{1}{\sqrt{15}}\delta_{a_1b_1}P_2(a_2b_2;c_2d_2)\\
T_{111}(a_1b_1;a_2b_2c_2d_2) &= \frac{1}{4}\epsilon_{a_1b_1r}\epsilon_{rts}\epsilon_{sb_2a_2}\epsilon_{td_2c_2}\\
T_{122}(a_1b_1;a_2b_2c_2d_2) &= \sqrt{\frac{8}{39}}\epsilon_{a_1b_1r}\epsilon_{rts}P_2(sm;a_2b_2)P_2(tm;c_2d_2)\\
T_{110}(a_1b_1;a_2b_2c_2d_2) &= \frac{1}{2\sqrt{3}}\epsilon_{a_1b_1r}\epsilon_{rb_2a_2}\delta_{c_2d_2}\\
T_{101}(a_1b_1;a_2b_2c_2d_2) &= \frac{1}{2\sqrt{3}}\epsilon_{a_1b_1r}\delta_{a_2b_2}\epsilon_{rd_2c_2}\\
T_{112}(a_1b_1;a_2b_2c_2d_2) &= \frac{1}{2}\sqrt{\frac{3}{5}}\epsilon_{a_1b_1r}\epsilon_{sb_2a_2}P_2(rs;c_2d_2)\\
T_{121}(a_1b_1;a_2b_2c_2d_2) &= \frac{1}{2}\sqrt{\frac{3}{5}}\epsilon_{a_1b_1r}\epsilon_{sb_2a_2}P_2(rs;a_2b_2)\\
T_{211}(a_1b_1;a_2b_2c_2d_2) &= \frac{1}{2}P_2(a_1b_1;rt)\epsilon_{ra_2b_2}\epsilon_{sc_2d_2}\\
T_{222}(a_1b_1;a_2b_2c_2d_2) &= 2\sqrt{\frac{3}{7}}P_2(a_1b_1;rt)P_2(ra;a_2b_2)P_2(st;c_2d_2)\\
T_{202}(a_1b_1;a_2b_2c_2d_2) &= \frac{1}{\sqrt{3}}P_2(a_1b_1;c_2d_2)\delta_{a_2b_2}\\
T_{220}(a_1b_1;a_2b_2c_2d_2) &= \frac{1}{\sqrt{3}}P_2(a_1b_1;a_2b_2)\delta_{c_2d_2}\\
T_{212}(a_1b_1;a_2b_2c_2d_2) &= \frac{1}{\sqrt{3}}P_2(a_1b_1;rt)\epsilon_{rsl}\epsilon_{lb_2a_2}P_2(st;c_2d_2)\\
T_{221}(a_1b_1;a_2b_2c_2d_2) &= \frac{1}{\sqrt{3}}P_2(a_1b_1;rt)\epsilon_{rsl}\epsilon_{td_2c_2}P_2(st;a_2b_2). \qquad \text{(A.12)}
\end{aligned}
$$

We decompose the group tensor $t_{2\to4}$ into these normalized transition tensors. With

$$t_{2\to4}(a_1b_1;a_2b_2c_2d_2) = \epsilon_{a_1la_2}\epsilon_{lmb_2}\epsilon_{mnc_2}\epsilon_{nb_1d_2} \qquad \text{(A.13)}$$

we obtain:

$$
\begin{aligned}
t_{2\to4} &= \frac{4}{\sqrt{3}}T_{000} - T_{011} + \sqrt{\frac{5}{3}}T_{022}\\
&+\frac{1}{2}T_{111} - \frac{1}{8}\sqrt{78}T_{122} - \frac{2}{\sqrt{3}}T_{110} - \frac{2}{\sqrt{3}}T_{101} - \frac{1}{2}\sqrt{\frac{5}{3}}T_{112} - \frac{1}{2}\sqrt{\frac{5}{3}}T_{121}
\end{aligned}
$$

$$+\frac{1}{2}T_{211} + \frac{1}{2}\sqrt{73}T_{222} - \frac{2}{\sqrt{3}}T_{202} - \frac{2}{\sqrt{3}}T_{220} + \frac{1}{2}\sqrt{3}T_{212} + \frac{1}{2}\sqrt{3}T_{221}. \qquad \text{(A.14)}$$

Next we adress the recoupling problem which now consists of two parts. First we consider the transition 3-reggeon $\to$ 4-reggeon (Fig.16). The coefficients are given in Table 3: the symbol (123) indicates that the lines "1", "2", and "3" result from a $2 \to 3$ transition etc. Next we we look at the four-reggeon final states (Fig.15). For the pairwise interaction in the four reggeon channel we list the coefficients in Tables 4a and b for the cases I=0 and I=1, resp. The notation is similar to that of Table 2, i.e. (12) denotes the pairwise interaction of the lines "1" and "2" etc. For brevity, we restrict ourselves from now on to total isospin $I = 0$ and $I = 1$ and do not present the numbers for the case $I = 2$.

Next we turn to the other coupling scheme (Fig.10b). Before we come to the definition of the normalized transition tensors, we need projection operators $P_{II_{23}}$ for $3 \to 3$ amplitudes (the coupling scheme is shown in Fig.4b). In addition to the six possibilities which we had for the $2 \to 3$ case above, we also need the case $(I, I_{23}) = (3, 2)$. The normalization condition is:

$$P_{II_{23}} \cdot P_{I'I'_{23}} = \delta_{I,I'}\delta_{I_{23},I'_{23}}P_{II_{23}}. \qquad \text{(A.15)}$$

Explicitly:

$$
\begin{aligned}
P_{01}(a_1b_1c_1;a_2b_2c_2) &= \frac{1}{6}\epsilon_{a_1b_1c_1}\epsilon_{a_2b_2c_2}\\
P_{10}(a_1b_1c_1;a_2b_2c_2) &= \frac{1}{3}\delta_{a_1a_2}\delta_{b_1c_1}\delta_{b_2c_2}\\
P_{11}(a_1b_1c_1;a_2b_2c_2) &= \frac{1}{4}\epsilon_{b_1c_1l}\epsilon_{a_1lr}\epsilon_{rsa_2}\epsilon_{sc_2b_2}\\
P_{12}(a_1b_1c_1;a_2b_2c_2) &= \frac{3}{5}P_2(b_1c_1;a_1r)P_2(a_2r;b_2c_2)\\
P_{21}(a_1b_1c_1;a_2b_2c_2) &= \frac{1}{2}\epsilon_{b_1c_1l}P_2(a_1l;a_2m)\epsilon_{mb_2c_2}\\
P_{22}(a_1b_1c_1;a_2b_2c_2) &= \frac{2}{3}P_2(b_2c_2;lm)\epsilon_{a_2ln}P_2(nm;rs)\epsilon_{a_2tr}P_2(ts;b_2c_2)\\
P_{32}(a_1b_1c_1;a_2b_2c_2) &= \delta_{a_1a_2}P_2(b_1c_1;b_2c_2) - \frac{3}{20}P_{12}(a_1b_1c_1;a_2b_2c_2) -\\
&\quad \frac{1}{12}P_{22}(a_1b_1c_1;a_2b_2c_2). \qquad \text{(A.16)}
\end{aligned}
$$

Now we are in the position to define the transition tensors $T_{I,I_{234},I_{34}}$ which are normalized according to:

$$T_{I,I_{234},I_{34}} T_{I',I'_{234},I'_{34}} = \delta_{II'}\delta_{I_{234},I'_{234}}\delta_{I_{34},I'_{34}} P_I. \tag{A.17}$$

In components, these tensors are:

$$\begin{aligned}
T_{010}(a_1b_1;a_2b_2c_2d_2) &= \frac{1}{\sqrt{27}}\delta_{a_1b_1}\delta_{a_2b_2}\delta_{c_2d_2}\\
T_{011}(a_1b_1;a_2b_2c_2d_2) &= \frac{1}{6}\delta_{a_1b_1}\delta_{a_2r}\epsilon_{b_2rs}\epsilon_{c_2sd_2}\\
T_{012}(a_1b_1;a_2b_2c_2d_2) &= \frac{1}{\sqrt{15}}\delta_{a_1b_1}P_2(a_2b_2;c_2d_2)\\
T_{101}(a_1b_1;a_2b_2c_2d_2) &= \frac{1}{2\sqrt{3}}\epsilon_{a_1b_1a_2}\epsilon_{b_2c_2d_2}\\
T_{110}(a_1b_1;a_2b_2c_2d_2) &= \frac{1}{2\sqrt{3}}\epsilon_{a_1b_1r}\epsilon_{a_2rb_2}\delta_{c_2d_2}\\
T_{111}(a_1b_1;a_2b_2c_2d_2) &= \frac{1}{4}\epsilon_{a_1b_1r}\epsilon_{a_2rs}\epsilon_{b_2st}\epsilon_{c_2td_2}\\
T_{112}(a_1b_1;a_2b_2c_2d_2) &= \frac{1}{2}\sqrt{\frac{3}{5}}\epsilon_{a_1b_1r}\epsilon_{a_2rs}P_2(b_2s;c_dd_2)\\
T_{121}(a_1b_1;a_2b_2c_2d_2) &= \frac{1}{2}\sqrt{\frac{3}{5}}\epsilon_{a_1b_1r}P_23(a_2r;b_2s)\epsilon_{sd_2c_2}\\
T_{122}(a_1b_1;a_2b_2c_2d_2) &= \frac{1}{\sqrt{5}}\epsilon_{a_1b_1r}P_2(a_2r;ln)\epsilon_{b_2lm}P_2(mn;c_2d_2)\\
T_{210}(a_1b_1;a_2b_2c_2d_2) &= \frac{1}{\sqrt{3}}P_2(a_1b_1;rt)\epsilon_{b_2rs}\epsilon_{c_2sd_2}\\
T_{211}(a_1b_1;a_2b_2c_2d_2) &= \frac{1}{2}P_2(a_1b_1;a_2r)\epsilon_{b_2rs}\epsilon_{c_2sd_2}\\
T_{212}(a_1b_1;a_2b_2c_2d_2) &= \sqrt{\frac{3}{5}}P_2(a_1b_1;a_2r)P_2(rb_2;c_2d_2)\\
T_{221}(a_1b_1;a_2b_2c_2d_2) &= \frac{1}{\sqrt{3}}P_2(a_1b_1;rt)\epsilon_{a_2rs}P_2(st;b_2l)\epsilon_{c_2ld_2}\\
T_{222}(a_1b_1;a_2b_2c_2d_2) &= \frac{2}{3}P_2(a_1b_1;rt)\epsilon_{a_2rs}P_2(st;lm)\epsilon_{b_2ln}P_2(mn;c_2d_2)\\
T_{232}(a_1b_1;a_2b_2c_2d_2) &= \sqrt{\frac{5}{7}}P_2(a_1b_1;rt)P_{32}(a_2rt;b_2mn)P_2(mn;c_2d_2).
\end{aligned} \tag{A.18}$$

We again decompose the group tensor $t_{2\to4}$ into these normalized transition tensors::

$$\begin{aligned}
t_{2\to4} &= 4\sqrt{3}T_{010} - T_{011} + \sqrt{\frac{5}{3}}T_{012}\\
&\quad - 2\sqrt{\frac{5}{3}}T_{101} - 2\sqrt{\frac{5}{3}}T_{110} + \frac{1}{2}T_{111} - \frac{1}{2}\sqrt{\frac{5}{3}}T_{112} - \frac{1}{2}\sqrt{\frac{5}{3}}T_{121} - \frac{1}{2}\sqrt{5}T_{122}\\
&\quad - \frac{1}{2\sqrt{3}}T_{210} + \frac{1}{2}T_{211} - \frac{1}{2}\sqrt{\frac{5}{3}}T_{212} + \frac{1}{2}\sqrt{3}T_{221} + \frac{3}{2}T_{222}.
\end{aligned} \tag{A.19}$$

Next we have to calculate the recoupling coefficients. We proceed in the same way as for the previous coupling scheme. In Table 5 we present the coefficients for the transitions 3-reggeons $\to$ 4-reggeons, using the same notations as in Table 3. Finally, Tables 6a and 6b contain the coefficients for the pairwise interactions in the four-reggeon final states. The notations are analogous to those of Tables 4a and 4b.

Table 1

$$
\begin{aligned}
T_{2\to 2} &= \int \frac{dj}{2\pi i} s^{j} \xi_{j} F(j,t) \\
T_{2\to 3} &= \int \frac{dj_1}{2\pi i} \int \frac{dj_2}{2\pi i} \Big(s^{j_1} s_{bc}^{j_2-j_1} \xi_{j_1} \xi_{j_2;j_1} F_1(j_1,j_2,t_1,t_2,\eta) + s^{j_2} s_{ab}^{j_1-j_2} \xi_{j_2} \xi_{j_1;j_2} F_2(j_1,j_2,t_1,t_2,\eta) \Big) \\
T_{2\to 4} &= \int \frac{dj_1}{2\pi i} \int \frac{dj_2}{2\pi i} \int \frac{dj_3}{2\pi i} \Big(s^{j_1} s_{bcd}^{j_2-j_1} s_{cd}^{j_3-j_2} \xi_{j_1} \xi_{j_2;j_1} \xi_{j_3;j_2} F_1(j_1,j_2,j_3,t_1,t_2,t_3,\eta_b,\eta_c) \\
&\quad + s^{j_3} s_{abc}^{j_2-j_3} s_{ab}^{j_1-j_2} \xi_{j_3} \xi_{j_2;j_3} \xi_{j_1;j_2} F_3(j_1,j_2,j_3,t_1,t_2,t_3,\eta_b,\eta_c) \\
&\quad + s^{j_2} s_{ab}^{j_1-j_2} s_{cd}^{j_3-j_2} \xi_{j_2} \xi_{j_1;j_2} \xi_{j_3;j_2} F_2(j_1,j_2,j_3,t_1,t_2,t_3,\eta_b,\eta_c) \\
&\quad + s^{j_3} s_{abc}^{j_1-j_3} s_{bc}^{j_2-j_1} \xi_{j_3} \xi_{j_1;j_3} \xi_{j_2;j_1} F_{31}(j_1,j_2,j_3,t_1,t_2,t_3,\eta_b,\eta_c) \\
&\quad + s^{j_1} s_{bcd}^{j_3-j_1} s_{bc}^{j_2-j_3} \xi_{j_1} \xi_{j_3;j_1} \xi_{j_2;j_3} F_{13}(j_1,j_2,j_3,t_1,t_2,t_3,\eta_b,\eta_c) \Big) \\
T_{3\to 3} &= \int \frac{dj_1}{2\pi i} \int \frac{dj_2}{2\pi i} \int \frac{dj_3}{2\pi i} \Big(s^{j_1} s_{b2}^{j_2-j_1} s_{cd}^{j_3-j_2} \xi_{j_1} \xi_{j_2;j_1} \xi_{j_3;j_2} F_1(j_1,j_2,j_3,t_1,t_2,t_3,\eta_b,\eta_c) \\
&\quad + s^{j_3} s_{ac}^{j_2-j_3} s_{1b}^{j_1-j_2} \xi_{j_3} \xi_{j_2;j_3} \xi_{j_1;j_2} F_3(j_1,j_2,j_3,t_1,t_2,t_3,\eta_b,\eta_c) \\
&\quad + s^{j_2} s_{1b}^{j_1-j_2} s_{cd}^{j_3-j_2} \xi_{j_2} \xi_{j_1;j_2} \xi_{j_3;j_2} F_2(j_1,j_2,j_3,t_1,t_2,t_3,\eta_b,\eta_c) \\
&\quad + s^{j_3+j_1-j_2} s_{ac}^{j_2-j_3} s_{b2}^{j_2-j_1} \xi_{j_2;j_3} \xi_{j_2;j_1} \xi_{j_1;j_3;j_2} F_{31}(j_1,j_2,j_3,t_1,t_2,t_3,\eta_b,\eta_c) \\
&\quad + s_{ac}^{j_1} s_{1ac}^{j_2-j_3-j_1} s_{b2}^{j_3} \xi_{j_1} \xi_{j_3} \xi_{j_2;j_1;j_3} F_{13}(j_1,j_2,j_3,t_1,t_2,t_3,\eta_b,\eta_c) \Big) \\
T_{3\to 3} &= \int \frac{dj}{2\pi i} \int \frac{dj_1}{2\pi i} \int \frac{dj_2}{2\pi i} s^{j_1} s^{j_2} s_{\chi}^{j} \xi_{j_1} \xi_{j_2} \xi_{j;j_1;j_2} F(j,j_1,j_2,t,t_1,t_2) \\
\xi_{j} &= \frac{e^{-i\pi j}+\tau}{\sin \pi j} \\
\xi_{j_1;j_2} &= \frac{e^{-i\pi(j_1-j_2)}+\tau_1\tau_2}{\sin \pi(j_1-j_2)} \\
\xi_{j_1 j_3;j_2} &= \frac{e^{-i\pi(j_1+j_3-j_2)}+\tau_1\tau_2\tau_3}{\sin \pi(j_1+j_3-j_2)} \\
\eta_b &= (q_1-q_2)^2 + M^2
\end{aligned}
$$

Table 2

I	I'_{23}	I_{23}	(12)	(23)	(13)
0	1	1	-1	-1	-1
1	0	0		-2	
	1	0	$\frac{2}{\sqrt{3}}$		$-\frac{2}{\sqrt{3}}$
	2	0			
	0	1	$\frac{2}{\sqrt{3}}$		$-\frac{2}{\sqrt{3}}$
	1	1	$-\frac{1}{2}$	-1	$-\frac{1}{2}$
	2	1	$\sqrt{\frac{5}{12}}$		$-\sqrt{\frac{5}{12}}$
	0	2			
	1	2	$\sqrt{\frac{5}{12}}$		$-\sqrt{\frac{5}{12}}$
	2	2	$-\frac{3}{2}$	1	$-\frac{3}{2}$
2	1	1	$\frac{1}{2}$	-1	$\frac{1}{2}$
	2	1	$\frac{\sqrt{3}}{2}$		$-\frac{\sqrt{3}}{2}$
	1	2	$\frac{\sqrt{3}}{2}$		$-\frac{\sqrt{3}}{2}$
	2	2	$-\frac{1}{2}$	1	$-\frac{1}{2}$

Table 3

I	I'_{23}	$I_{12}I_{34}$	(123)	(234)	(134)	(124)
0	1	00	$-2\sqrt{\frac{2}{3}}$	$-2\sqrt{\frac{2}{3}}$	$2\sqrt{\frac{2}{3}}$	$2\sqrt{\frac{2}{3}}$
	1	11	$\frac{1}{\sqrt{2}}$	$\frac{1}{\sqrt{2}}$	$\frac{1}{\sqrt{2}}$	$\frac{1}{\sqrt{2}}$
	1	22	$-\sqrt{\frac{5}{6}}$	$-\sqrt{\frac{5}{6}}$	$\sqrt{\frac{5}{6}}$	$\sqrt{\frac{5}{6}}$
1	0	11	$\sqrt{\frac{2}{3}}$	$\sqrt{\frac{2}{3}}$	$\frac{1}{\sqrt{6}}$	$\sqrt{\frac{2}{3}}$
	1		$-\frac{1}{\sqrt{8}}$	$-\frac{1}{\sqrt{8}}$		$-\frac{1}{\sqrt{8}}$
	2		$\frac{1}{2}\sqrt{56}$	$\frac{1}{2}\sqrt{56}$	$-\sqrt{56}$	$-\frac{1}{2}\sqrt{56}$
1	0	22			$\frac{1}{4}\sqrt{13}$	
	1		$\frac{1}{8}\sqrt{39}$	$\frac{1}{8}\sqrt{39}$		$\frac{1}{8}\sqrt{39}$
	2		$\frac{3}{8}$	$\frac{3}{8}$	$-\frac{1}{4}\sqrt{\frac{13}{5}}$	$\frac{3}{8}$
1	0	10		$-\frac{2}{3}\sqrt{2}$		
	1		$\sqrt{\frac{2}{3}}$	$2\sqrt{\frac{2}{3}}$	$-\sqrt{\frac{2}{3}}$	$-\sqrt{\frac{2}{3}}$
	2				$\frac{1}{3}\sqrt{10}$	
1	0	01	$-\frac{2}{3}\sqrt{2}$	$-\sqrt{2}$	$\sqrt{2}$	$\frac{2}{3}\sqrt{2}$
	1		$\sqrt{\frac{2}{3}}$	$\frac{1}{2}\sqrt{\frac{2}{3}}$	$-\frac{1}{2}\sqrt{\frac{2}{3}}$	$\sqrt{\frac{2}{3}}$
	2		$\frac{1}{3}\sqrt{10}$	$\frac{1}{6}\sqrt{10}$	$-\frac{1}{6}\sqrt{10}$	$-\frac{1}{3}\sqrt{10}$
1	0	12			$-\frac{1}{3}\sqrt{\frac{5}{2}}$	
	1		$\frac{1}{2}\sqrt{56}$	$-\frac{1}{2}\sqrt{56}$	$\sqrt{56}$	$-\frac{1}{2}\sqrt{56}$
	2		$-\frac{3}{4}\sqrt{2}$	$\frac{3}{4}\sqrt{2}$	$-\frac{1}{3}\sqrt{2}$	$-\frac{3}{4}\sqrt{2}$
1	0	21	$\frac{2}{3}\sqrt{\frac{5}{2}}$	$-\frac{2}{3}\sqrt{\frac{5}{2}}$	$-\frac{1}{3}\sqrt{\frac{5}{2}}$	$-\frac{2}{3}\sqrt{\frac{5}{2}}$
	1		$\frac{1}{2}\sqrt{\frac{5}{6}}$	$-\frac{1}{2}\sqrt{\frac{5}{6}}$	$-\sqrt{\frac{5}{6}}$	$\frac{1}{2}\sqrt{\frac{5}{6}}$
	2		$-\frac{1}{12}\sqrt{2}$	$\frac{1}{12}\sqrt{2}$	$-\frac{1}{3}\sqrt{2}$	$\frac{1}{12}\sqrt{2}$

Table 4a

I	$I'_{12}I'_{34}$	$I_{12}I_{34}$	(12)	(34)	(23)	(14)	(13)	(24)
0	00	00	-2	-2				
	11	00			$\frac{2}{\sqrt{3}}$	$\frac{2}{\sqrt{3}}$	$-\frac{2}{\sqrt{3}}$	$-\frac{2}{\sqrt{3}}$
	22	00						
	00	11			$\frac{2}{\sqrt{3}}$	$\frac{2}{\sqrt{3}}$	$-\frac{2}{\sqrt{3}}$	$-\frac{2}{\sqrt{3}}$
	11	11	-1	-1	$-\frac{1}{2}$	$-\frac{1}{2}$	$-\frac{1}{2}$	$-\frac{1}{2}$
	22	11			$\frac{1}{2}\sqrt{\frac{5}{3}}$	$\frac{1}{2}\sqrt{\frac{5}{3}}$	$-\frac{1}{2}\sqrt{\frac{5}{3}}$	$-\frac{1}{2}\sqrt{\frac{5}{3}}$
	00	22						
	11	22			$\frac{1}{2}\sqrt{\frac{5}{3}}$	$\frac{1}{2}\sqrt{\frac{5}{3}}$	$-\frac{1}{2}\sqrt{\frac{5}{3}}$	$-\frac{1}{2}\sqrt{\frac{5}{3}}$
	22	22	1	1	$\frac{2}{3}$	$\frac{2}{3}$	$\frac{2}{3}$	$\frac{2}{3}$

Table 4b

I	$I'_{12}I'_{34}$	$I_{12}I_{34}$	(12)	(34)	(23)	(14)	(13)	(24)
1	11	11	-1	-1	$-\frac{1}{4}$	$\frac{1}{4}$	$-\frac{1}{4}$	$-\frac{1}{4}$
	22				$\frac{5}{\sqrt{78}}$	$\frac{5}{\sqrt{78}}$	$-\frac{5}{\sqrt{78}}$	$-\frac{5}{\sqrt{78}}$
	10				$\frac{1}{\sqrt{3}}$	$-\frac{1}{\sqrt{3}}$	$\frac{1}{\sqrt{3}}$	$-\frac{1}{\sqrt{3}}$
	01				$\frac{1}{\sqrt{3}}$	$-\frac{1}{\sqrt{3}}$	$-\frac{1}{\sqrt{3}}$	$\frac{1}{\sqrt{3}}$
	12				$\frac{1}{4}\sqrt{\frac{5}{3}}$	$-\frac{1}{4}\sqrt{\frac{5}{3}}$	$\frac{1}{4}\sqrt{\frac{5}{3}}$	$-\frac{1}{4}\sqrt{\frac{5}{3}}$
	21				$\frac{1}{4}\sqrt{\frac{5}{3}}$	$-\frac{1}{4}\sqrt{\frac{5}{3}}$	$-\frac{1}{4}\sqrt{\frac{5}{3}}$	$\frac{1}{4}\sqrt{\frac{5}{3}}$
	11	22			$\frac{1}{8}\sqrt{78}$	$\frac{1}{8}\sqrt{78}$	$-\frac{1}{8}\sqrt{78}$	$-\frac{1}{8}\sqrt{78}$
	22		1	1	$-\frac{5}{4}$	$-\frac{5}{4}$	$-\frac{5}{4}$	$-\frac{5}{4}$
	10							
	01							
	12				$\frac{3}{16}\sqrt{\frac{26}{5}}$	$-\frac{3}{16}\sqrt{\frac{26}{5}}$	$-\frac{3}{16}\sqrt{\frac{26}{5}}$	$\frac{3}{16}\sqrt{\frac{26}{5}}$
	21				$\frac{3}{16}\sqrt{\frac{26}{5}}$	$-\frac{3}{16}\sqrt{\frac{26}{5}}$	$\frac{3}{16}\sqrt{\frac{26}{5}}$	$-\frac{3}{16}\sqrt{\frac{26}{5}}$
1	11	10			$\frac{1}{\sqrt{3}}$	$-\frac{1}{\sqrt{3}}$	$\frac{1}{\sqrt{3}}$	$-\frac{1}{\sqrt{3}}$
	22							
	10		-1	-2				
	01				$-\frac{2}{3}$	$-\frac{2}{3}$	$\frac{2}{3}$	$\frac{2}{3}$
	12							
	21				$\frac{1}{3}\sqrt{5}$	$\frac{1}{3}\sqrt{5}$	$-\frac{1}{3}\sqrt{5}$	$-\frac{1}{3}\sqrt{5}$
	11	01			$\frac{1}{\sqrt{3}}$	$-\frac{1}{\sqrt{3}}$	$-\frac{1}{\sqrt{3}}$	$\frac{1}{\sqrt{3}}$
	22							
	10				$-\frac{2}{3}$	$\frac{2}{3}$	$\frac{2}{3}$	$\frac{2}{3}$
	01		-2	-1				
	12				$\frac{1}{3}\sqrt{5}$	$\frac{1}{3}\sqrt{5}$	$\frac{1}{3}\sqrt{5}$	$\frac{1}{3}\sqrt{5}$
	21							
	11	12			$\frac{1}{4}\sqrt{\frac{5}{3}}$	$-\frac{1}{4}\sqrt{\frac{5}{3}}$	$\frac{1}{4}\sqrt{\frac{5}{3}}$	$-\frac{1}{4}\sqrt{\frac{5}{3}}$
	22				$\sqrt{\frac{5}{26}}$	$-\sqrt{\frac{5}{26}}$	$-\sqrt{\frac{5}{26}}$	$\sqrt{\frac{5}{26}}$
	10							
	01				$\frac{1}{3}\sqrt{5}$	$\frac{1}{3}\sqrt{5}$	$-\frac{1}{3}\sqrt{5}$	$-\frac{1}{3}\sqrt{5}$
	12		-1	1	$-\frac{3}{4}$	$-\frac{3}{4}$	$-\frac{3}{4}$	$-\frac{3}{4}$
	21				$-\frac{1}{12}$	$-\frac{1}{12}$	$\frac{1}{12}$	$\frac{1}{12}$
	11	21			$\frac{1}{4}\sqrt{\frac{5}{3}}$	$-\frac{1}{4}\sqrt{\frac{5}{3}}$	$-\frac{1}{4}\sqrt{\frac{5}{3}}$	$\frac{1}{4}\sqrt{\frac{5}{3}}$
	22				$\sqrt{\frac{5}{26}}$	$-\sqrt{\frac{5}{26}}$	$\sqrt{\frac{5}{26}}$	$-\sqrt{\frac{5}{26}}$
	10				$\frac{1}{3}\sqrt{5}$	$\frac{1}{3}\sqrt{5}$	$-\frac{1}{3}\sqrt{5}$	$-\frac{1}{3}\sqrt{5}$
	01							
	12				$-\frac{1}{12}$	$-\frac{1}{12}$	$\frac{1}{12}$	$\frac{1}{12}$
	21		1	-1	$-\frac{3}{4}$	$-\frac{3}{4}$	$-\frac{3}{4}$	$-\frac{3}{4}$

Table 5

I	I'_{23}	$I_{234}I_{34}$	(123)	(234)	(134)	(124)
0	1	10	$-2\sqrt{\frac{2}{3}}$	$-2\sqrt{\frac{2}{3}}$	$2\sqrt{\frac{2}{3}}$	$2\sqrt{\frac{2}{3}}$
	1	11	$\frac{1}{\sqrt{2}}$	$\frac{1}{\sqrt{2}}$	$\frac{1}{\sqrt{2}}$	$\frac{1}{\sqrt{2}}$
	1	12	$-\frac{1}{2}\sqrt{\frac{10}{3}}$	$-\frac{1}{2}\sqrt{\frac{10}{3}}$	$\frac{1}{2}\sqrt{\frac{10}{3}}$	$\frac{1}{2}\sqrt{\frac{10}{3}}$
1	0	01		$\sqrt{2}$		
	1	01	$\sqrt{\frac{2}{3}}$		$-\sqrt{\frac{2}{3}}$	$\sqrt{\frac{2}{3}}$
	2	01				
1	0	10			$-\frac{2}{3}\sqrt{2}$	
	1	10	$\sqrt{\frac{2}{3}}$	$2\sqrt{\frac{2}{3}}$	$-\sqrt{\frac{2}{3}}$	$-\sqrt{\frac{2}{3}}$
	2	10			$\frac{10}{3}\sqrt{10}$	
1	0	11	$2\sqrt{\frac{2}{3}}$		$-\sqrt{\frac{2}{3}}$	$-2\sqrt{\frac{2}{3}}$
	1	11	$-\frac{1}{2\sqrt{2}}$	$-\frac{1}{\sqrt{2}}$	$-\frac{1}{2\sqrt{2}}$	$-\frac{1}{2\sqrt{2}}$
	2	11	$-\frac{1}{2}\sqrt{\frac{5}{6}}$		$-\frac{1}{2}\sqrt{\frac{5}{6}}$	$-\frac{1}{2}\sqrt{\frac{5}{6}}$
1	0	12			$\frac{1}{3}\sqrt{10}$	
	1	12	$\frac{1}{2}\sqrt{\frac{5}{6}}$	$\sqrt{\frac{5}{6}}$	$-\frac{1}{2}\sqrt{\frac{5}{6}}$	$\frac{1}{2}\sqrt{\frac{5}{6}}$
	2	12	$\frac{3}{4}\sqrt{2}$		$\frac{1}{6\sqrt{2}}$	$\frac{3}{4}\sqrt{2}$
1	0	21				
	1	21	$\frac{1}{2}\sqrt{\frac{5}{6}}$		$-\frac{1}{2}\sqrt{\frac{5}{6}}$	$\frac{1}{2}\sqrt{\frac{5}{6}}$
	2	21	$\frac{3}{4}\sqrt{2}$	$\frac{1}{2}\sqrt{2}$	$-\frac{3}{4}\sqrt{2}$	$-\frac{3}{4}\sqrt{2}$
1	0	22				
	1	22	$\sqrt{\frac{5}{8}}$		$\sqrt{\frac{5}{8}}$	$-\sqrt{\frac{5}{8}}$
	2	22	$-\sqrt{\frac{3}{8}}$	$\sqrt{\frac{3}{2}}$	$-\sqrt{\frac{3}{8}}$	$-\sqrt{\frac{3}{8}}$

Table 6a

I	$I'_{234}I'_{34}$	$I_{234}I_{34}$	(12)	(34)	(23)	(14)	(13)	(24)
0	10	010	-2	-2				
	11				$\frac{2}{\sqrt{3}}$	$\frac{2}{\sqrt{3}}$	$-\frac{2}{\sqrt{3}}$	$-\frac{2}{\sqrt{3}}$
	12							
	10	011			$\frac{2}{\sqrt{3}}$	$\frac{2}{\sqrt{3}}$	$-\frac{2}{\sqrt{3}}$	$-\frac{2}{\sqrt{3}}$
	11		-1	-1	$-\frac{1}{2}$	$-\frac{1}{2}$	$-\frac{1}{2}$	$-\frac{1}{2}$
	12				$\frac{1}{2}\sqrt{\frac{5}{3}}$	$\frac{1}{2}\sqrt{\frac{5}{3}}$	$-\frac{1}{2}\sqrt{\frac{5}{3}}$	$-\frac{1}{2}\sqrt{\frac{5}{3}}$
	10	012						
	11				$\frac{1}{2}\sqrt{\frac{5}{3}}$	$\frac{1}{2}\sqrt{\frac{5}{3}}$	$-\frac{1}{2}\sqrt{\frac{5}{3}}$	$-\frac{1}{2}\sqrt{\frac{5}{3}}$
	12		1	1	$-\frac{3}{2}$	$-\frac{3}{2}$	$-\frac{3}{2}$	$-\frac{3}{2}$

Table 6b

I	$I'_{234}I'_{34}$	$I_{234}I_{34}$	(12)	(34)	(23)	(14)	(13)	(24)
1	01	01		-2	-1			-1
	10					$\frac{1}{3}$	$-\frac{1}{3}$	
	11		$\frac{1}{\sqrt{3}}$			$-\frac{1}{2\sqrt{3}}$	$-\frac{1}{2\sqrt{3}}$	
	12					$-\frac{1}{6\sqrt{5}}$	$\frac{1}{6\sqrt{5}}$	
	21							
	22							
	01	10				$\frac{4}{3}$	$-\frac{4}{3}$	
	10		-1	-2				
	11				$\sqrt{2}$	$\frac{1}{\sqrt{2}}$	$-\frac{1}{\sqrt{2}}$	$-\sqrt{2}$
	12							
	21					$-\frac{1}{\sqrt{5}}$	$\frac{1}{\sqrt{5}}$	
	22							
	01	11	$\frac{4}{\sqrt{3}}$			$-\frac{2}{\sqrt{3}}$	$-\frac{2}{\sqrt{3}}$	
	10				$\frac{2}{\sqrt{3}}$	$\frac{1}{\sqrt{3}}$	$-\frac{1}{\sqrt{3}}$	$-\frac{2}{\sqrt{3}}$
	11		$-\frac{1}{2}$	-1	$-\frac{1}{2}$	$-\frac{1}{4}$	$-\frac{1}{4}$	$-\frac{1}{2}$
	12				$\frac{1}{2}\sqrt{\frac{5}{3}}$	$\frac{1}{4}\sqrt{\frac{5}{3}}$	$-\frac{1}{4}\sqrt{\frac{5}{3}}$	$-\frac{1}{2}\sqrt{\frac{5}{3}}$
	21		$\frac{1}{2}\sqrt{\frac{3}{5}}$			$-\frac{1}{4}\sqrt{\frac{3}{5}}$	$-\frac{1}{4}\sqrt{\frac{3}{5}}$	
	22					$-\frac{3}{4\sqrt{5}}$	$\frac{3}{4\sqrt{5}}$	
	01	12				$-\frac{1}{3\sqrt{20}}$	$\frac{1}{3\sqrt{20}}$	
	10							
	11				$\frac{1}{2}\sqrt{\frac{5}{3}}$	$\frac{1}{4}\sqrt{\frac{5}{3}}$	$-\frac{1}{4}\sqrt{\frac{5}{3}}$	$-\frac{1}{2}\sqrt{\frac{5}{3}}$
	12		$\frac{1}{2}$	1	$-\frac{3}{2}$	$-\frac{3}{4}$	$-\frac{3}{4}$	$-\frac{3}{2}$
	21					$\frac{1}{20}$	$-\frac{1}{20}$	
	22		$2\sqrt{3}$			$-\sqrt{3}$	$-\sqrt{3}$	
	01	21						
	10					$-\frac{5}{9}\sqrt{5}$	$\frac{5}{9}\sqrt{5}$	
	11		$\frac{5}{6}\sqrt{\frac{5}{3}}$			$-\frac{5}{12}\sqrt{\frac{5}{3}}$	$-\frac{5}{12}\sqrt{\frac{5}{3}}$	
	12					$\frac{5}{36}$	$-\frac{5}{36}$	
	21		$-\frac{3}{2}$	-1	$\frac{1}{2}$	$-\frac{3}{4}$	$-\frac{3}{4}$	$\frac{1}{2}$
	22				$\frac{1}{2}\sqrt{3}$	$\frac{1}{4}\sqrt{3}$	$-\frac{1}{4}\sqrt{3}$	$-\frac{1}{2}\sqrt{3}$
	01	22						
	10							
	11					$-\frac{5}{12}\sqrt{\frac{5}{3}}$	$\frac{5}{12}\sqrt{\frac{5}{3}}$	
	12		$\frac{5}{2\sqrt{3}}$			$-\frac{5}{4\sqrt{3}}$	$-\frac{5}{4\sqrt{3}}$	
	21				$\frac{1}{2}\sqrt{3}$	$\frac{1}{4}\sqrt{3}$	$-\frac{1}{4}\sqrt{3}$	$-\frac{1}{2}\sqrt{3}$
	22		$-\frac{1}{2}$	1	$-\frac{1}{2}$	$-\frac{5}{4}$	$-\frac{5}{4}$	$-\frac{1}{2}$

References

[1] J.Bartels, *Nucl.Phys.* **B151**, 293(1979).

[2] J.Bartels, *Nucl.Phys.* **B175**, 365(1980).

[3] A.R.White, ANL-HEP-PR-90-28 and references therein.

[4] J.Bartels, *Acta Phys.Pol.* **B11**, 281(1980).

[5] A.R.White, *Nucl.Phys.B (Proc.Suppl.)* **12**, 190(1990) (Proceedings of the International Conference on Elastic and Diffraction Scattering 1989, ed. M.M.Block and A.R.White) and references therein.

[6] V.N.Gribov and L.N.Lipatov, *Sov.Journ.Nucl.Phys.* **15**, 438 and 675 (1972).

[7] G.Altarelli and G.Parisi, *Nucl.Phys.* **126**, 297(1977).

[8] Yu.L..Dokshitser, *Sov.Phys.JETP* **46**, 641(1977).

[9] L.V.Gribov, E.M.Levin, and M.G.Ryskin, *Phys. Rep.* **100**, 1 (1982)

[10] J.Bartels, DESY 90-153 and to be published in *Particle World.*

[11] A.Ringwald, *Nucl.Phys.* **B330**, 1(1990).

[12] V.V.Khoze and A.Ringwald, CERN Preprint CERN-TH-5912/90.

[13] V.V.Khoze and A.Ringwald, CERN Preprint CERN-TH-5990/91.

[14] A.H.Mueller, Columbia Preprint CU-TP-512 (1991).

[15] E.A.Kuraev, L.N.Lipatov, V.S.Fadin, *Sov.Phys.JETP* **44**, 443(1976).

[16] E.A.Kuraev, L.N.Lipatov, V.S.Fadin, *Sov.Phys.JETP* **45**, 199(1977).

[17] Ya.Ya.Balitzky, L.N.Lipatov *Sov.Jour.Nucl.Phys.* **28**, 822(1978).

[18] Ya.Ya.Balitzky, L.N.Lipatov *JETP Letters* **30**, 355(1979).

[19] L.N.Lipatov, *Sov.Phys.JETP* **63**, 904(1986) and references therein.

[20] C.Y.Lo and H.Cheng, *Phys.Rev.* **D13**, 1131(1976); *Phys.Rev.* **D15**, 2959(1977).

[21] J.Bartels, *Phys.Rev.* **D11**, 2977 and 2989 (1975).

[22] H.D.I.Abarbanel, J.Bartels, J.B.Bronzan, and D.Sidhu, *Phys.Rev.* **D12**, 2459(1975).

[23] H.D.I.Abarbanel, J.B.Bronzan, R.L.Sugar, and A.R.White, *Phys.Rep.* **21**, 119(1975).

[24] L.N.Lipatov, *Nucl.Phys.B (Proc.Suppl.)* **18C**, 6 (1991) (Proceedings of the DESY Topical Meeting on the Small-x Behavior 1990, ed.A.Ali and J.Bartels).

[25] A.R.White, *Intern.Journal of Modern Physics* **A6**, 1(1991) and references therein.

Figure Captions

Fig. 1: Graphical illustration of the leading-lns approximation. The notation follows I and II.

(a) Eq.(2.1) drawn as a reggeon diagram;

(b) the group structure of the $2 \to n$ amplitude: each vertex has a group tensor ϵ_{abc} (indices counterclockwise), and a line between two adjacent vertices indicates summation over the (identical) indices.

Fig. 2: Reggeon diagrams arising from the unitarity equation (2.4).

(a) The partial wave belonging to (2.4).

(b) The two-particle $\to$ two-reggeon amplitude which belongs to the partial wave in Fig.2a.

(c) Graphical illustration of the bootstrap equation (2.9).

Fig. 3: Graphical illustration of the double energy discontinuities (a) $disc_s disc_{s_{ab}}$ and (b) $disc_s disc_{s_{bc}}$. In contrast to the other reggeon diagrams, produced particles are depicted by full lines. Cutting off the particle vertices at (a) the left or (b) the right end, one is lead to define two-particle $\to$ three-reggeon vertices. Their integral equation is illustrated in (c).

Fig. 4: Coupling scheme of angular momentum and SU(2) quantum numbers for (a) the two-particle $\to$ three-reggeon vertex and (b) the three-reggeon $\to$ three-reggeon vertex.

Fig. 5: Illustration of the "bootstrap" equation (2.19).

Fig. 6: Illustration of the amplitude $D_3^{(10;-+)}$ (see the discussion after (2.27)).

Fig. 7: Examples of energy nonconserving reggeon amplitudes: the arrows mark the "last" vertex before the separation of the two branches: it is this vertex, where reggon energy is not conserved. Case (a) belongs to the triple Regge limit (cf.Fig.13). Case (b) is a generalization of Fig.3a. Figs.7c and d illustrate the solutions (2.37) and (2.43), resp.

Fig. 8: Illustration of the partial wave $F_{\cdot}^{(21;--)}$ (a) and the cut production vertex of (2.53) (b).

Fig. 9: Diagrams representing new real parts of $T_{2\to 2}$ (see the discussion in section 3). The maximal number of reggeons in the t-channel is three.
(a) reggeon diagrams without any "contraction" of lines.
(b) The same diagrams in the $(I=1, \tau=-)$ channel.
(c) The same diagrams in the even signature (I=0 or 2) channel; the (23) subsystem is constrained to the $(I=1, \tau=-)$ state.

Fig. 10: The two different coupling schemes of the two- particle $\to$ four-reggeon vertex.

Fig. 11: Integral equation of the two-particle $\to$ four-reggeon vertex. In the last two terms the summation symbol implies summation over all pairwise interactions.

Fig. 12: Diagrams for $T_{2\to 2}^{(nnl)}$ (see the discussion before (4.1)). Arrows mark those vertices where the number of reggeon lines changes.

Fig. 13: Reggeon diagrams illustrating the two-particle $\to$ four-reggeon amplitudes D_4 with three independent reggeon energy variables. They are obtained from the triple-energy discontinuity in the triple-Regge limit. The integral equations are given in (4.4)-(4.9). In Fig 13b the same diagrams are redrawn for the case (000,+++).

Fig. 14: The first fan diagram of Gribov, Levin, and Ryskin. All wavy lines denote gluons.

Fig. 15: Illustration of the recoupling problem: in D_3 on the left side the system (2'3') has definite isospin, whereas multiplication with the D_3 on the rhs requires definite isospin in the (1'2') system.

Fig. 16: Illustration of the recoupling problem in D_4: the pairwise interaction of reggeons "2" and "3" has definite isospin in the (23)-subsystem, whereas D_4 has been reduced into irreducible representations in the (12) and the (34)-subsystems.

Fig. 17: momenta for the kernel $K_{2\to n}$ in eq.(5.1).

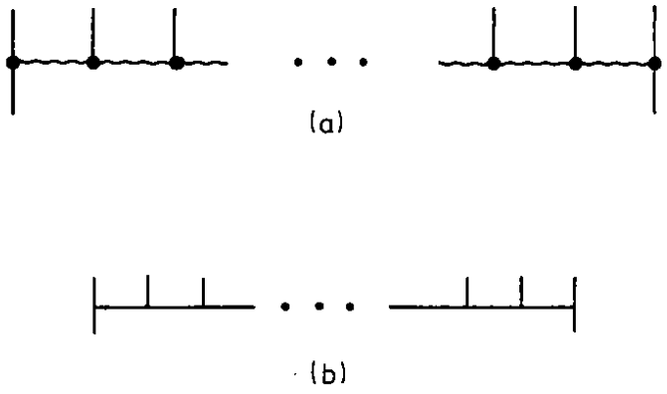

Fig. 1

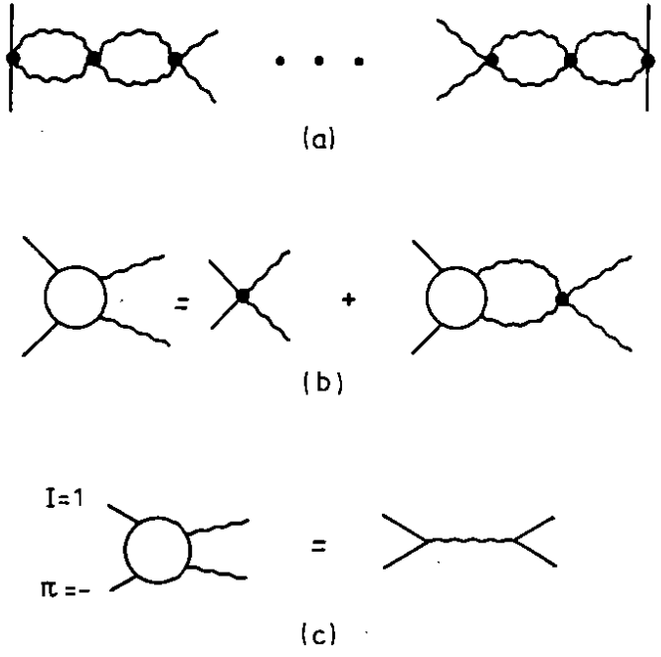

Fig. 2

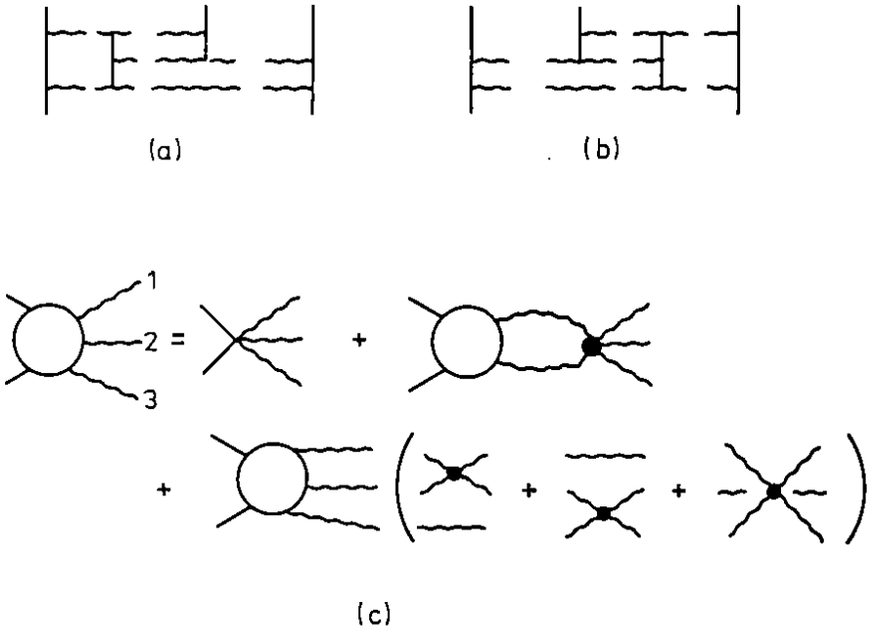

Fig. 3

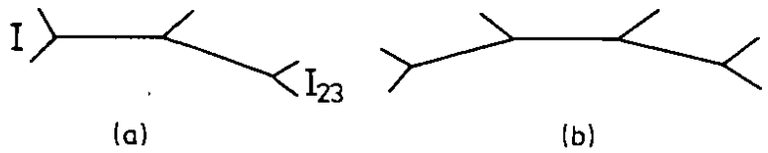

Fig.4

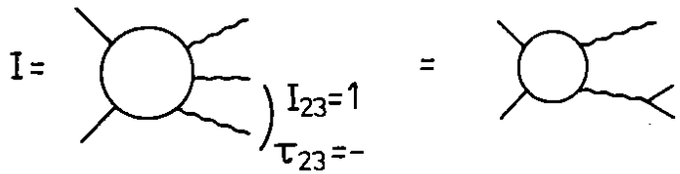

Fig. 5

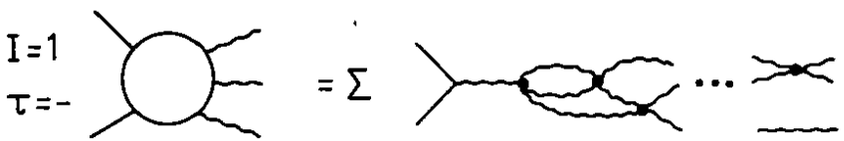

Fig. 6

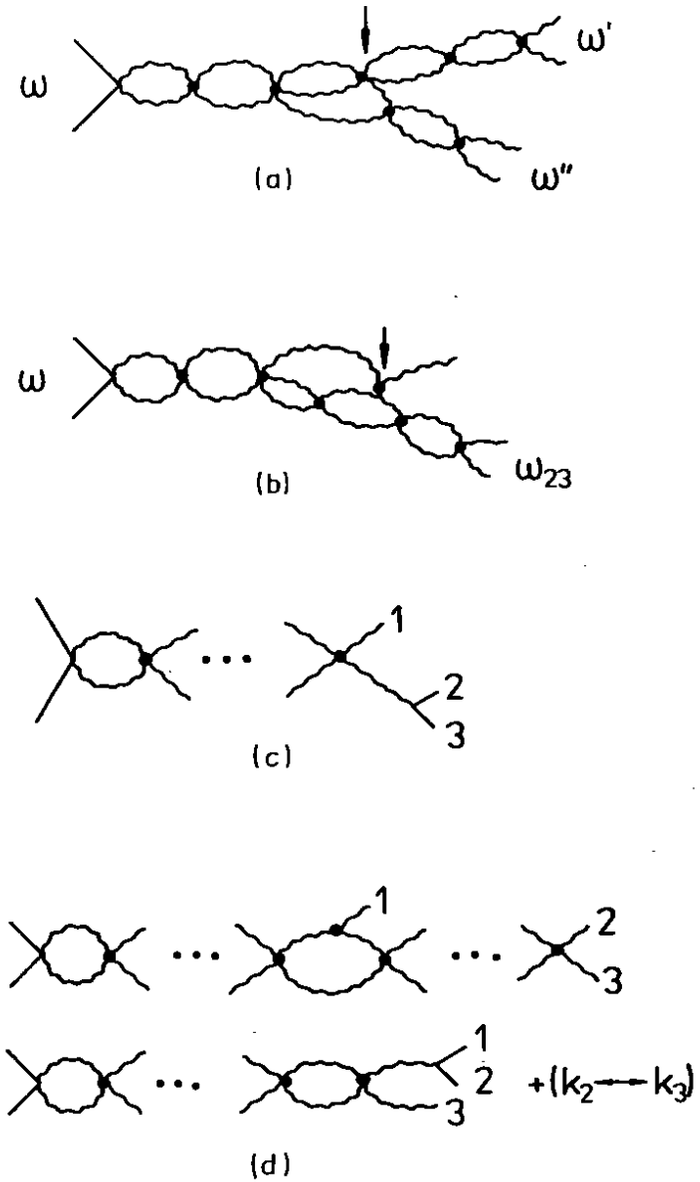

Fig.7

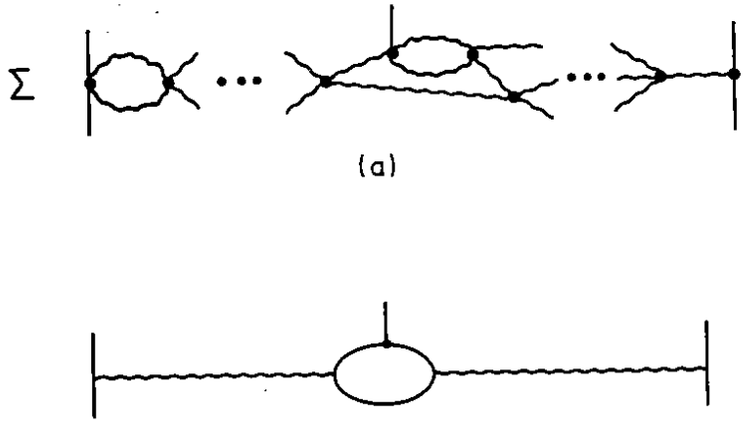

Fig.8

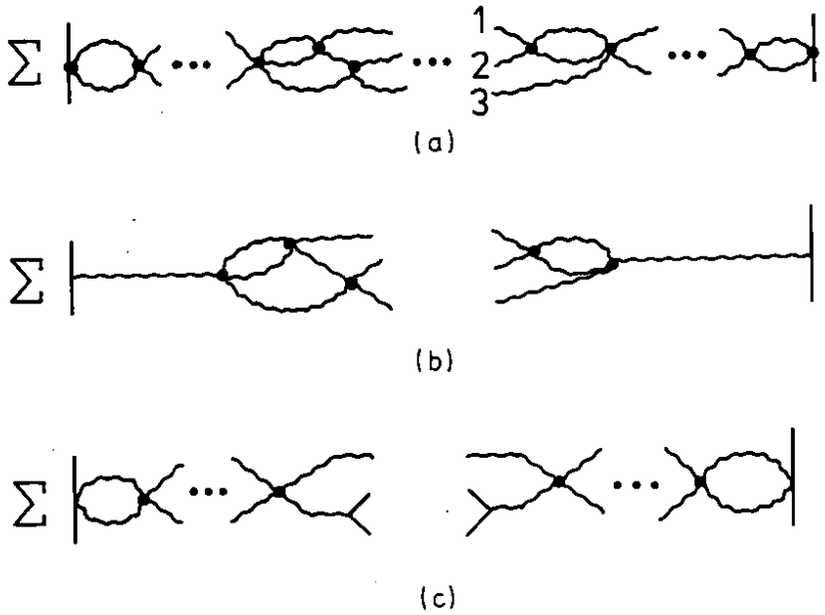

Fig.9

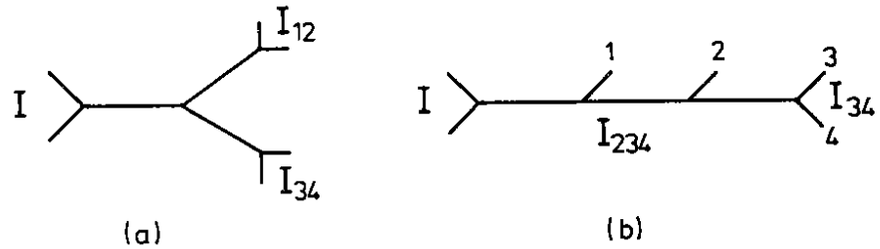

Fig.10

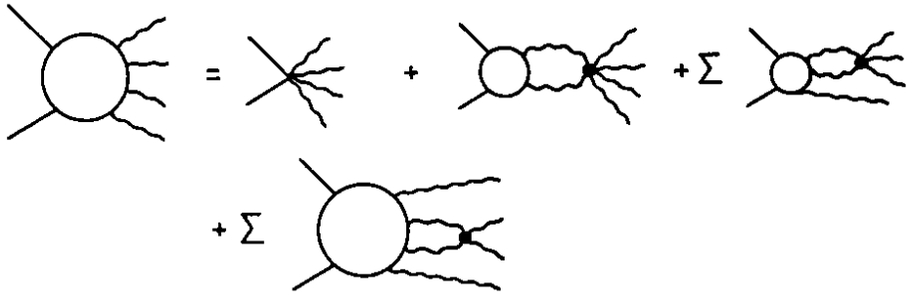

Fig.11

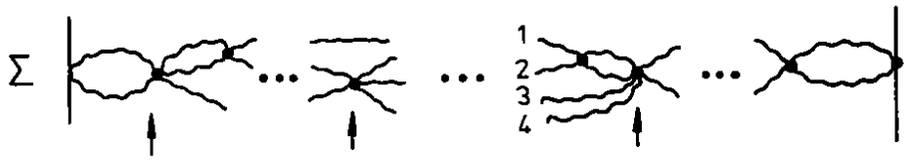

Fig.12

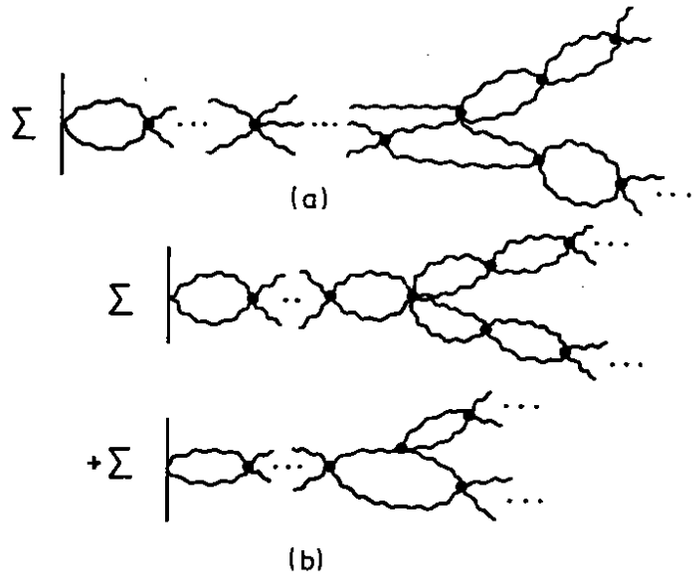

Fig.13

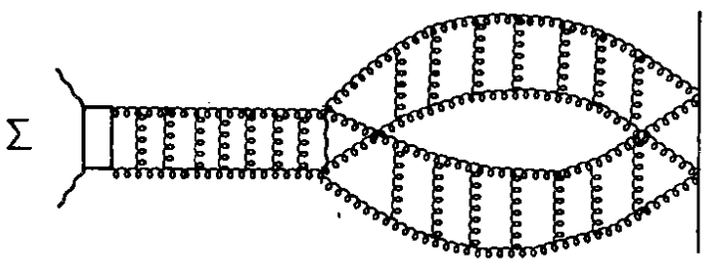

Fig.14

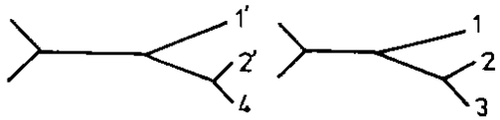

Fig.15

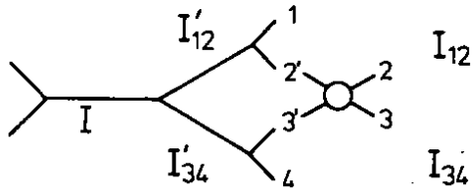

Fig.16

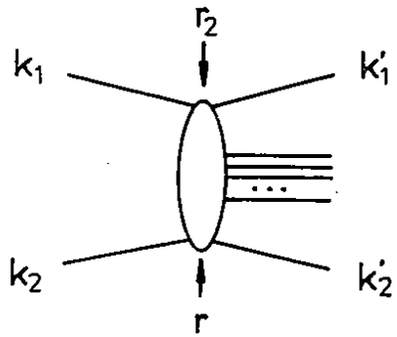

Fig.17